HYDRODYNAMIC MODELING FOR FLOOD HAZARD ASSESSMENT IN TELOMOYO CATCHMENT, CENTRAL JAVA, INDONESIA

Thesis submitted to the Double Degree M.Sc. Programme, Gadjah Mada University and Faculty of Geo-Information Science and Earth Observation, University of Twente
in partial fulfillment of the requirement for the degree of Master of Science in
Planning and Management of Coastal and Watershed

By :
FRIETA DAMAYANTI
08/279239/PGE/00774
25301

Supervisors :

1. **Dr. Djati Mardiatno, M.Si. (UGM)**
2. **Dr. Danang Sri Hadmoko, M.Sc. (UGM)**
3. **Dr. Menno Straatsma (ITC)**
4. **Dr. Dinand Alkema (ITC)**

DOUBLE DEGREE M.Sc. PROGRAMME
GADJAH MADA UNIVERSITY
FACULTY OF GEO-INFORMATION AND EARTH OBSERVATION
UNIVERSITY OF TWENTE
2011

ABSTRACT

Flooding is considered as one of the most devastating events in many parts of the world. In terms of its frequency and distribution, river flooding remains as a frequent disaster that has to be faced by civilization in the floodplain. Due to the periodical occurrence and adverse impact that may be generated, flood risk management is necessary to conduct. Flood hazard assessment is the preliminary step in conducting the flood risk management.

A coupled 1D2D hydrodynamic modeling has become a popular practical method in flood hazard assessment due to its advantage in predicting the flood events which did not occur in history. This modeling helps to understand the flood hazard and serves a tool which also useful in understanding the effect of mitigation measures. The flood model was based on four diffent retun periods (2 yr, 5 yr, and 25 yr). Digital elevation model (DEM) is substantially important in conducting such flood model. Geostatistical analysis was preferred to do DEM generation. Three interpolation methods were used in this study and the results were compared. The Simple Kriging is the best geostatistical predictor since it embedded the least SD, RMSE.

The result of the flood model show that the flood, either from low magnitude (2 yr) and high magnitude (25 yr) only inundate 15% of the study area. The positive relationship of the inundation area and flood magnitude was identified. The comparison of the flood model and the observed data in term of the flood depth showed 35 cm differences.

Keywords: hydrodynamic model, DEM, kriging, flood hazard

ACKNOWLEDGEMENT

Alhamdulillahirabbil'alamiin...praise to Allah for giving me an incredibly precious life and strength to have this experience. I would have not been this though to complete my studies without His hand and bless.

I would like to thank Departemen Pendidikan Nasional RI who has funded my study through Beasiswa Unggulan framework.

I sincerely thank to Prof. Dr. Junun Sartohadi for the opportunity to have a great experience to study abroad.

I sincerely thank to my supervisors, Dr. M.W. Straatsma and Dr. D. Alkema, for their dedication and precious time to guide me throughout my entire research.

I thank to Dr. Djati Mardiatno, M.Si. and Dr. Danang Sri Hadmoko for their advises and the guidance.

I thank also to Pak Tom (Tom Loran), Pak Voskuil (Robert Voskuil), and Pak David (Dr. D.G. Rossiter) for all the support and help.

I would like to thank to Eric Quincieu (BCEOM), Pak Rio Nugroho (Public Work Office) and Pak Jumadi (BPDAS Probolo) for the data and discussion.

Many thanks to all AES student especially Geohazard people Sarah Tumuhairwe, Haydar Youssif Hussin, Darwin Edmund Riguer, Syams Nashrullah, Pooyan Rahimy, and Samjana Ghimire. Thank you for the friendship and the support.

Many thanks for Indonesian student in ITC for giving me a very nice family atmosphere and also for LUPIS (Landuse Policy and Sustainable Development) Project crew thank you for the understanding by letting me to finish this thesis.

The greatest debt is owed to my beloved family, my mother, my father, my sisters and brothers. They convinced me to keep tough and always pray the best for me. I would like to thank them and dedicate this for them. Last, my deepest gratitude to Adit for always being there for me, helping me out to get through this.

Contents

Tables

Figures

Graph

1. Introduction

1.1. Research Background

Flooding is considered as one of the most devastating events in many parts of the world. In terms of its frequency and distribution, river flooding remains as a frequent disaster that has to be faced by civilization in the floodplain. Smith and Ward (1998) defined "the real risk of flood stems from the likelihood that a major hazardous event will occur unexpectedly and that it will impact negatively on people and their welfare". Flooding is getting more frequently reported in the mass media both the minor events that will be forgotten soon and major events that will be remembered for many years, such as massive flooding in Pakistan recently that killed 1200 people and more than 14 million people affected (UN-OCHA, 2010).

The global flood risk has been increasing as the world's population is rapidly growing. The consequences of rapid population growth are the increasing of demand for settlement, food, resources. Kundwezicz and Menzel (2003) noted that the world's changing can be attributed to the change of three systems, terrestrial, social-economy, and climatic system. In order to accommodate the needs due to the population growth, floodplain and river levee have been occupied by placing new buildings and other infrastructures. Land use change represents the disturbed terrestrial system. It triggers hydrological change by increasing the impervious area and leave a little space for water storage. The development and urbanization of the floodplain has attracted people to live in and investing economic properties there. The river dike and other river protection have convinced the society toward the safety. The social-economic system has been changed in the floodplain and so has been the people's exposure to the flood hazard. The global change cannot be separated with the change in climatic system. Climate variability, regardless of global warming, may change the atmospheric circulation and lead to the prolonged rainfall which then increases the probability of flooding to occur.

Due to the periodical occurrence and adverse impact that may be generated, flood risk management is necessary to conduct. Basically, flood risk analysis consists of two aspect, flood hazard (extreme events and associated probabilities) and the consequences of flooding (property damage) (Apel et al., 2004). Various flood characteristics are required for effective flood hazard assessment such as flood historical event, flood depth, flow velocities, and extent. The last three characteristics can be obtained from a flood model.

Nowadays, hydrodynamic modeling has become a popular practical method in flood hazard assessment due to its advantage in predicting the flood events which did not occur in history. This modeling helps to understand the flood hazard and serves a tool which also useful in understanding the effect of mitigation measures. Hydrodynamic models route the water over the Digital Elevation Model (DEM) forced by upstream boundary conditions such as a meteorological forcing, or a hydrograph and downstream boundary conditions of water levels. These models are available in many types nowadays, from simple 1D models to complex 3D models, taking flow direction into account (Prachansri, 2007).

To gain a comprehensive flood risk analysis, all relevant flood scenarios and their associated probabilities should be incorporated. The probabilities attached in the flood hazard have raised the uncertainties to be analyzed further (Apel et al., 2004). The uncertainty could exist due to either the spatial variability (aleatory uncertainty) or incomplete knowledge (epistemic uncertainty). Data-driven model such hydrodynamic takes many non-stationary parameters into account. The flood hazard may be changing over time since the dynamic input data. Identifying the uncertainties and incorporates them into analysis step supports in decision making by providing many preferences. *Uncertainty is of relevance to decision makers because of its potential influence on preference orderings* (Hall & Solomatine, 2010).

1.2. Research Problem

Uncertainty incorporated in a flood modeling may come from the input data such as discharge, roughness, digital elevation model (DEM), channels, and dikes. These uncertainties will be inherited during the modeling process and after the model result obtained. Rainfall-runoff model has been used as input data in the flood modeling. Such model is able to represent the basin response in form of the runoff towards the incoming rainfall. This hydrological apparently seems ideal for the flood modeling, but the catchment morphometry exhibit the model uncertainty. Neuhold et al. (2009) incorporated river morphological changes as the uncertainty in the flood risk assessment. The uncertainty of the DEM used in the flood model is rarely considered (Wechsler, 2003). The adjustment of surface roughness is preferred to do the uncertainty analysis.

Uncertainty attached in DEM may be produced by the error during the elevation survey, inadequate point density, or during the interpolation process (S. P. Wechsler, 2007). Provision of detailed DEM is a considerable issue in many areas due to the economic factors. Though DEM can be derived from on line-satellite imageries which is free of cost, the resolution both horizontal and vertical is not detailed enough to represent the flat terrain topography. ASTER-GDEM with 30 m horizontal resolution is the best freely available DEMs for the users in internet. However the vertical accuracy is more essential. The vertical accuracy of ASTER-GDEM is up to 20 meter at 95% confidence level (ASTER GDEM Validation Team, 2009). In this study area, such problem is found. Inadequate topographic accuracy may increase the model uncertainty. The "uncertainty" term is raised in this work due to no sufficient detailed field measurement, thus there is lack of the real value.

Investigation of DEM error on many applications has been world-wide discussed. The most common way to study the DEM error is by investigating its effect in the topographic parameters as done by many researchers (Hunter and Goodchild, 1997; Wechsler & Kroll, 2006). Effect of spot height interpolation error on grid size of DEM and hydrologic parameters has been investigated by Lagacherie et al. (1996) and Casas et al. (2006). Based on the review, the effect of DEM error on the flood hazard mapping is not yet known. The DEMs error propagating in the flood model and the probability incorporated in the different flood magnitude might perform different pattern of the flood hazard but it is needed to investigate in detail.

1.3. Research Objectives and Research Question

The main objective of this research is to assess the effect of DEM uncertainty on flood hazard in a data poor environment. The specific objectives and related research questions are listed below.

1) To create a DEM for flood modeling
   - Which interpolation method gives the best result for the DEM generation?
   - How should the error of interpolated DEM be assessed?
2) To model the flood behavior through hydrodynamic modeling
   - Which areas are to be likely inundated by the different return period floods?
   - What is the significant change of flood behavior with the changing flood return periods?
3) To derive the flood hazard from different return period?
   - Is there any systematic pattern of the flood extent for the different return period?

1.4. General Methodology

This research was started conceptual building by doing the literature review for associated topic and followed by data collection on the study area in South Central Java, Indonesia. The ancillary data were collected from the Public Work Office. During the data collection interview with the local people was also conducted to validate the information about the past event flood. Every data obtained was first explored before it is used in further analysis. The elevation point as the most substantial data for this research was used to construct DEM. The DEM construction and related topics were mainly done in R environment and exported to ILWIS. The generated DEM was adjusted with the elevated features such as road, railways, and river dike to get closer representation of the reality.

The geostatistical analysis in this study was used R environment. R is free software environment for statistical and graphics and use S language. Basically, R needs script to be able to do the analysis. R provides many standard statistical analysis and many advanced statistical method (Bivand, 2008).

The flood behavior was simulated in1D2D SOBEK modeling and calibrated with the flood depth information collected from the interviews with the local community in 6 subdistricts (Gombong, Kuwarasan, Karanganyar, Adimulyo, Buayan, and Puring). Adjustment of Manning's value data set was also conducted for the calibration. The flood modeling was based on baseline scenario and uncertainty scenario. The baseline scenario used the general DEM which was assumed to be error free and the uncertainty scenario use the noisy DEM.

The last step is the assessment of the flood modeling based on the baseline scenario and the uncertainty scenario. The flood hazard was derived from combination of flood depth and flood velocity. The investigation done in this final step is for the pattern exists in the different flood scenario and the probability of cells to be inundated. The general workflow of the research is presented in Figure 1-1.

1.5. Problem and Limitation of the Study

During the research process, several constraints were found such as the data availability, inadequate information of certain data, and the time limitation. Data availability is the most basic needs of a research. Working in the area with sparse data is a challenge. Unavailable detail discharge and rainfall data for the past event flood need many assumptions and approach to be built in order to undertake this constraint.

A proper technique to introduce the noise was done very thorough due to the unavailable error information of the elevation point. Documented information about how the elevation was measured and the associated error of the data set is essential. Literature review on the related topics is an alternative to make an assumption and approach the error value. The third constraint found in the study is related to pixel size and time required for the simulation. Since the coverage area of this study is relatively large hence the grid size was limited to 50 meter. Smaller grid size will increase the time computation and affect model stability.

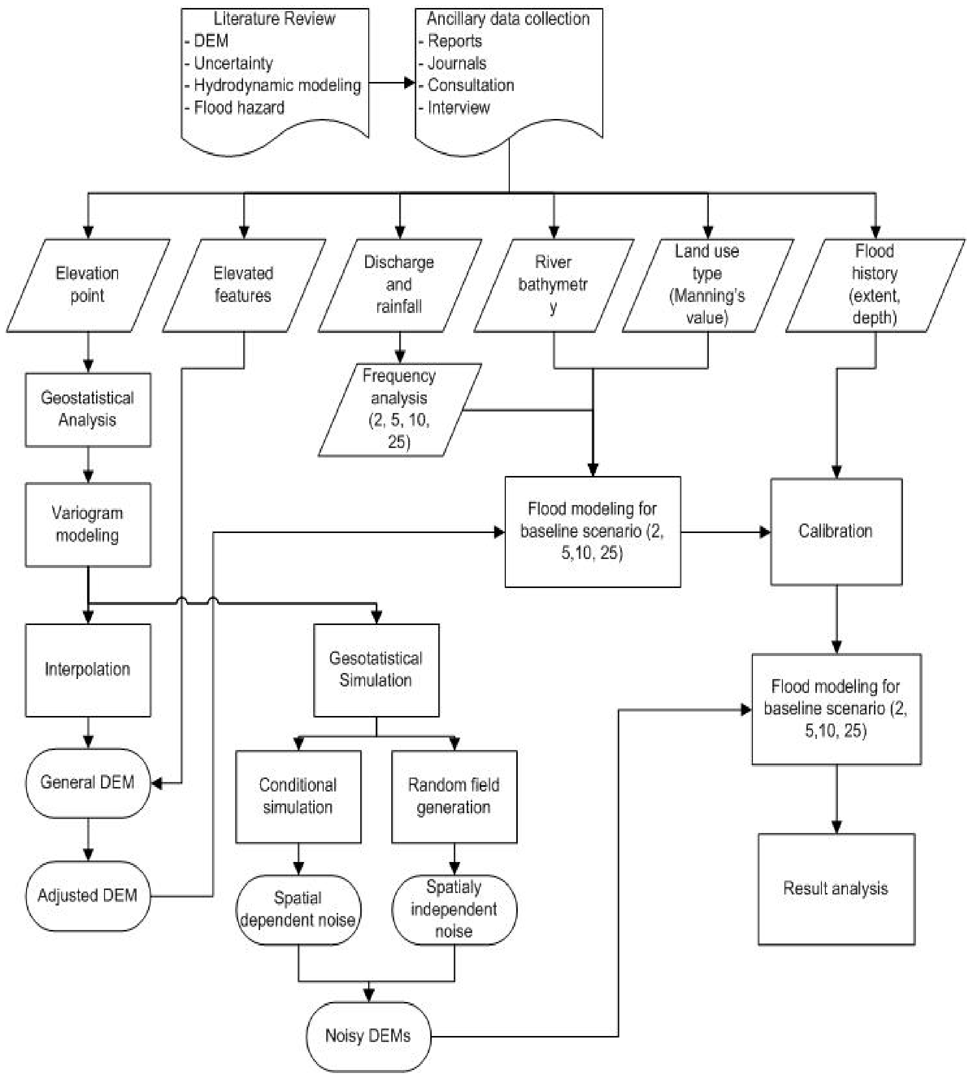

Figure 1-1. The general workflow of the research

1.6. Thesis Outline

Chapter 1

The first chapter is an introduction which comprises of background of the research, problem, objectives and research questions. This last components is sort of guidance of this research.

Chapter 2

Study area is described in this chapter. Physical condition of the study area is explained including geomorphology and geology, soil condition, and existing land use. Climatic and meteorological conditions are also discussed in this chapter.

Chapter 3

In this chapter, literature review is presented to back up all the procedures taken in this research. It includes the information of what have been done by the other researchers and what is still left uninvestigated.

Chapter 4

This chapter is attributed to the DEM related topic. Overall methodology of DEM generation is defined followed by the result. The prediction error is investigated to identify the uncertainty. The quality of interpolated DEM is measured in accuracy assessment.

Chapter 5

This chapter addresses the second objective which focuses on the hydrodynamic modeling. The boundary setting is firstly conducted followed by schematization and at last carry out the model based on different return period of floods.

Chapter 6

The findings of the research are discussed in this chapter including the limitation and how to solve it.

Chapter 7

This chapter presents the conclusions derived from this research. Recommendations for the next research are proposed.

2. Study Area

The Telomoyo Catchment is located in Kebumen District, southern Central Java Province, at latitude 7° 31’ and 7° 47’ south and longitudes 109° 27’ and 109° 36’ east. It is about 420 km to south east of Jakarta, the capital city of Indonesia. This area is known of its agricultural commodity which contributes almost 35% of the Gross Domestic Product. Telomoyo Catchment is not densely populated with 995 people/km^2 and about 2429 people/km2 for city center, Gombong. This catchment extends over 509 km^2 and consists of several tributaries, i.e. Turus, Ketek, Karanganyar, Kemit, Gombong, and Jatinegara, coming from Serayu Hills in the northern part. A multipurpose reservoir named Sempor was constructed in 1970s and functioned to provide water for irrigating, generating electricity power, and supplying drinking water to the city of Gombong in the lower southern part (Figure 2.1).

Telomoyo Catchment has been facing flood related problems almost every year. The flooding mainly is caused by prolonged rainfall leading to dike breaks in some tributaries. Rivers in southern part of Java Island are characterized by the small distance between upper and lower stream, hence the water velocity is relatively high. The area suffered from a massive flood in November 2004. It was caused by the prolonged rainfall which led to the dike break Kemit River in Tegalsari Village, Adimulyo Subdistrict. The local government reported that this flood inundated three sub-districts, 160 ha of agricultural land, and 175 houses.

Telomoyo Catchment was a part flood management project called South Java Flood Control Sector Project from 1996 – 2007 and funded by the Asian Development Bank (ADB, 2007). The project was designated to address the adverse social effect social and economic losses caused by the floods. One of the scopes of the project was flood control and protection in which included river levee reinforcement along the Telomoyo, Ketek, Karanganyar, and Kemit Rivers; demolition of inadequate drainage structures and construction of suitable gated structures at the confluence of major drains into the rivers; and demolition of inadequate foot and village bridges and construction of suitable foot and village bridges. A flood model was also conducted in the project as a base of the flood management.

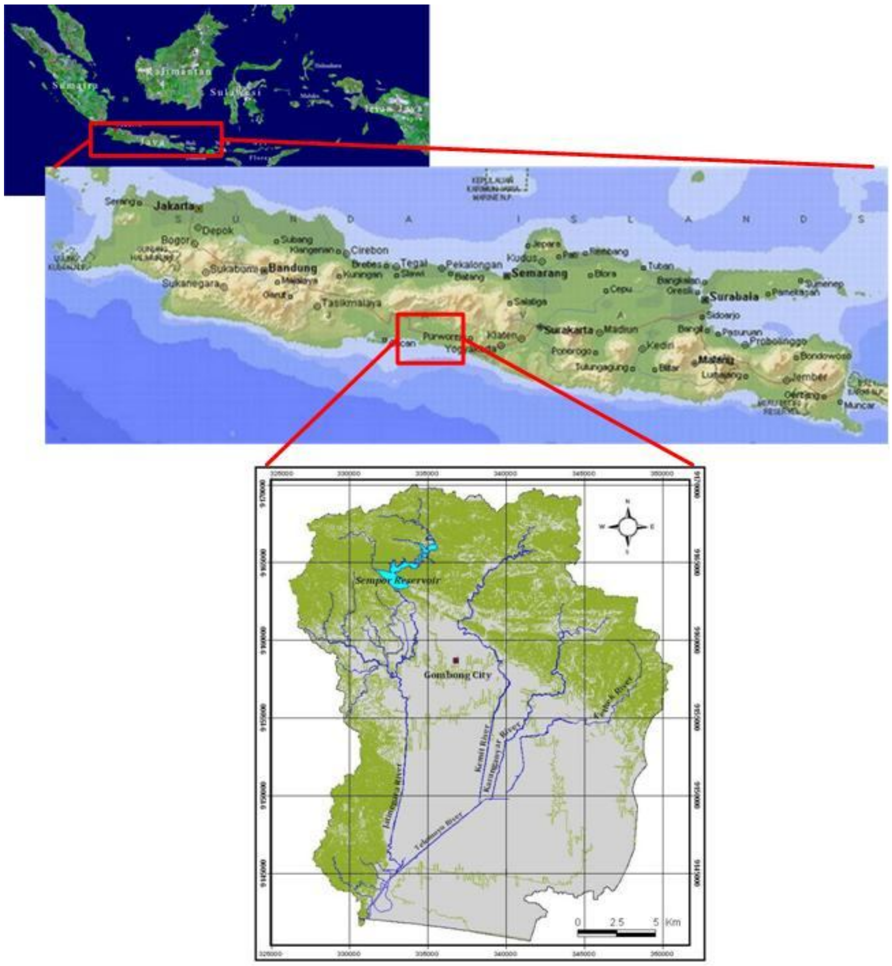

Figure 2-1. Location of Telomoyo Watershed, Central Java Province, Indonesia

2.1. Climate and Weather Condition

In general the climate in the study area is affected by the Monsoon and consists of rainy season (October – April) and dry season (May – September). Based on Schmidt-Fergusson Classification, the study area was categorized as Type B climate with 7 wet months (precipitation > 200 m) and three dry months (precipitation < 100 m) (Savitri, 2006). The average annual rainfall over the study area within 15 years (1990 – 2008) is

2971 mm. The minimum temperature is ranging from 14.2° to 23.5° C. The humidity is up to 70-85%.

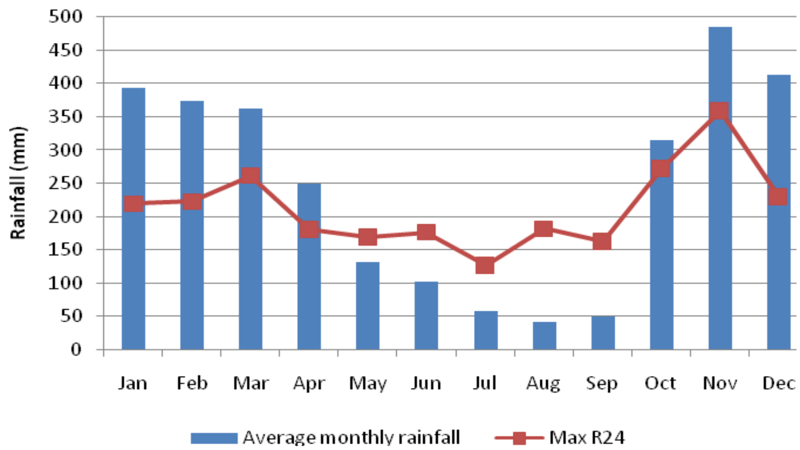

Figure 2-2. Rainfall pattern of Telomoyo Catchment within 15 years

Two peaks of rainfall (see Table 2.1) fell in the study area affected the duration of the flood reaching up to three days from November 6th to 8th 2004. The catchment responded the rainfall in form of water discharges which were recorded in six weirs (see Table 2.2). High peak discharges were reached in Sindut and Rowokawuk weir, while the other four weirs did not show the significant changes. The discharges in Bojong weir was stable due to the absence of over flow in the reservoir spillway although the rainfall recorded in Sempor was relatively high,

Table 2-1. Historical rainfall information for 2004 flood event

Rainfall Station	Nov 5th	Nov 6th	Nov 7th	Nov 8th	Nov 9th
Somogede	70	150	70	120	0
Rowokawuk	84	204	67	193	0
Watubarut	46	171	36	222	0
Gombong	27	177	37	207	0
Karanganyar	9	145	71	195	36
Sempor	60	153	31	148	0

Table 2-2. Historical water discharge information for 2004 flood event

Weir	Nov 5th	Nov 6th	Nov 7th	Nov 8th	Nov 9th
Kejawang	0	35.34	21.23	6.45	2.26
Sindhut	6.02	280	99.5	99.5	34.3
Rowokawuk	80.21	304	68.13	56.44	18.44
Watubarut	0	7.5	17.16	26.42	3.3
Bojong	2.48	2.48	2.48	2.48	2.48
Kedungkeji	1.67	8.37	1.67	2.18	1.67

2.2. Geomorphology and Geology

Telomoyo Catchment is divided into four geomorphologic units: 1) Serayu Mountainous Range in the northern part, 2) alluvial plain in the middle part, 3) coastal plain in the southern part, and 4) carbonate Karang Bolong Hills in the west known as South Gombong Karst. North and South Serayu Mountainous Range is separated by Serayu Depression in which several volcanic mountains developed. Thus the geological setting of this geomorphologic unit is tertiary pyroclastic sedimentary rock (Savitri, 2006). The changing of the mountainous geomorphologic unit to the alluvial plain is abrupt. The deflection of some rivers tributaries to east indicate a structural process has controlled the area.

The geological setting in the middle part is younger than mountainous range. The formation is generated from fluvial processes. The eroded material from the hilly area are transported and deposited in the alluvial plain. This geomorphologic unit is the most prominent in the study area. Very gentle slope steepness of the alluvial plain slows down the water flow due to the small river gradient. Being adjacent with the coastal plain in the south makes the alluvial plain sort of depression. The coastal plain in which beach ridges are located has higher elevation than the alluvial plain. The existing beach ridges behave as the natural protection from the flood. In the same coastal area, Karang Bolong carbonate hill is located in the west.

2.3. Soil

In term of flooding event, soil condition has contribution to the infiltration process and retaining the water. Sandy soil will behave differently with clay soil in draining the water. Table 2-3 shows that the study area is dominated by association of grey alluvial and grey-brown alluvial (41.35%). This soil type is affected by the fluvial processes and found in the middle part of the catchment. The flat terrain of catchment is controlled by the rivers. Alluvial soils, the so-called alluvium, are undeveloped and coarse textured soils. The ability to drain the water is supposed to be very useful in flood related problem. But the domination of paddy field apparently has turned the alluvium physical properties. Very intensive cultivation and watering process in the paddy field has created a hard soil structure and pad layer in the sub soil which then decrease the infiltration capacity of the soil. Pad layer forces the inundating water to stay longer on the surface. The agricultural cultivation in the upper catchment has caused a generic problem. Soil erosion as a consequence has moved the sediment to the lower part through the river transportation. This leads to the decreasing of river capacity as the river bed increases, hence the flood hazard becomes higher.

Table 2-3. Soil type of the study area

Soil type	Area (Km^2)	Area (%)
Association of Grey Alluvial and Grey-brown Alluvial	210.61	41.35
Complex Lithosol, Mediterranean and Rendzina	46.76	9.18
Reddish-dark brown Latosol	200.04	39.28
Grey Regosol	30.11	5.91
Complex Yellow-red Latosol, Brown Latosol, Yellow-red Podsolic	9.98	1.96
Complex Yellow-red Podsolic, Yellow Podsolic and Regosol	11.81	2.32
Total	509.32	100

2.4. Land use

Land use type contributes to the water infiltration and economic development of the society. Irrigated paddy field covers 29.68% of the study area. Based on Table 2.4, the study area apparently is not densely populated since settlement is relatively narrow (19%). Agriculture based land use types are more prominent in this study area.

Table 2-4. Distribution of land use type

Land use types	Area (Ha)	Percentage area (%)
Irrigated paddy field	15116	29.68
Rain-fed paddy field	3274	6.43
Dry-land agriculture	2128	4.18
Settlement	10129	19.89
Homestead	10704	21.02
Forest	7576	14.88
Bush	317	0.62
Beach	96	0.19
Others	1589	3.12
Total	50929	100

2.5. Data Description

The data description was done to identify the required data to reach the research objectives. The listed data in Table 2-5 were collected from the previous flood monitoring project, South Java Flood Control Sector Project (SJFCSP), conducted by Directorate General of Water Resources in 1997 - 2007.

To simulate the flood behavior, several ancillary data are required such as:

1. Flood depth information of 2004 event to validate the flood model;
2. Validated flood extent map of 2004 event to compare the flood extent resulted by the model;
3. Elevated features in the study area such as road, railways, and river dikes.

Table 2-5. List of available digital data

No	Data type	Method and source	Scale
1	Digital contour map contour interval 12.5 m	Digitized from topo map, National Survey and Mapping Agency	1 : 25000
2	River tributaries	Digitized from topo map, National Survey and Mapping Agency	1 : 25000
3	18827 spot heights, 100 m by 100 m intervals	Aerial photograph and field measurement	
4	River bathymetry	Detailed field measurement on 2001 – 2003, SJFCSP	
5	Flood extent of 2004 event	Public Work Office	1 : 25000
6	Discharge data	Public Work Office	Daily
7	Rainfall data	Public Work Office	Daily
8	Designed flood hydrograph for 2, 5, 10, and 25 years return period	Hydrological model, SJFCSP	
9	Designed maximum rainfall for 2, 5, 10, and 25 years return period	Frequency analysis, SJFCSP	
10	Landuse type	Derived from SPOT 5 year 2006, Geography Faculty, UGM	1 : 25000

2.5.1. Elevation Data

The elevation data were derived from the previous project SJFCSP. The data were prepared in 2002 and used to generate DEM. The coverage of the data, the so-called project area, was 208.73 km^2 and the mountainous area in the north ignored (see Figure 2-3). The written document of the elevation data was not available thus the metadata of the elevation point was derived from short interview with former staff. The point data was up scaled from 1 : 25000 scale topographic map. Aerial photos and detailed field measurement was used to produced spot height in 100 m x 100 m.

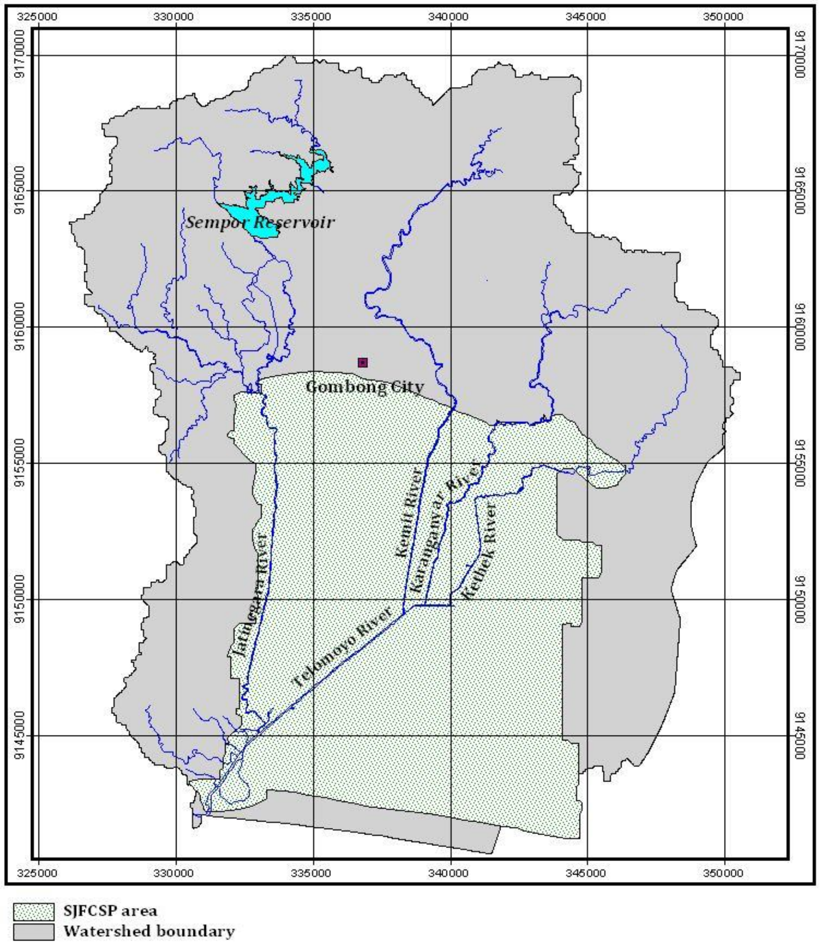

Figure 2-3. Coverage of the elevation data set used by SJFCSP in 2002

2.5.2. River Bathymetry

As was mentioned in the introduction of this chapter, the scope of SJFCSP work was to reinforce the river levee as the flood protection for the surrounding settlement. The reinforcement was done by elevating the old river dike and normalizing the river bed. The river bathymetry was designed and the post construction river dike was drawn (see Figure 2-4). The levee reinforcements were done on the Telomoyo tributaries including Jatinegara, Kemit, Karanganyar, and Kethek River and finished in 2003.

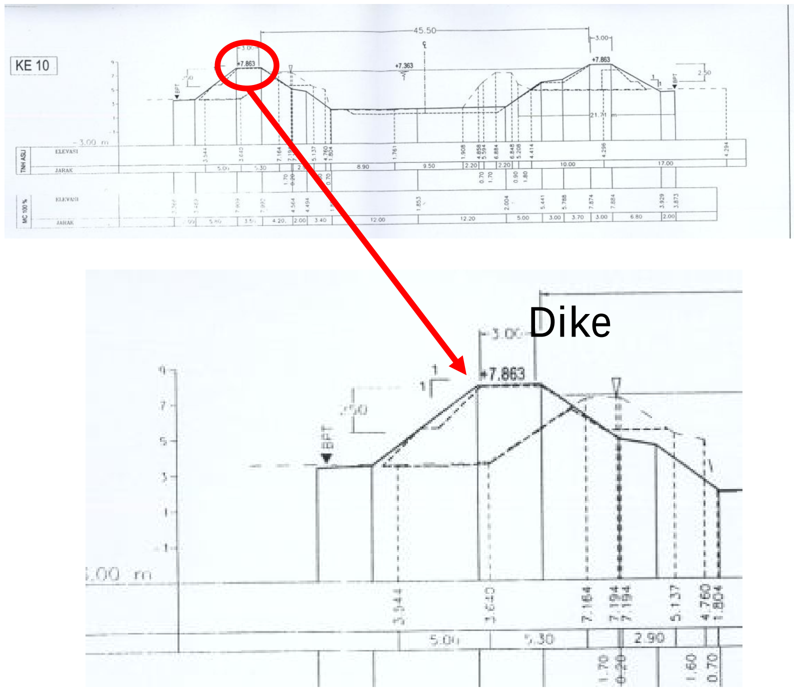

Figure 2-4. River levee reinforcement done by elevating the existing levee and normalizing the channel

2.5.3. Flood Extent

Flood extent map of 2004 event was generated based on the field visit by the Public Work Office. The map was derived from field visit right after the flood event took place. The horizontal accuracy for this map was about 5 to 7 meter since the survey used handheld GPS. This flood extent was validated by interviewing the local people during the fieldwork.

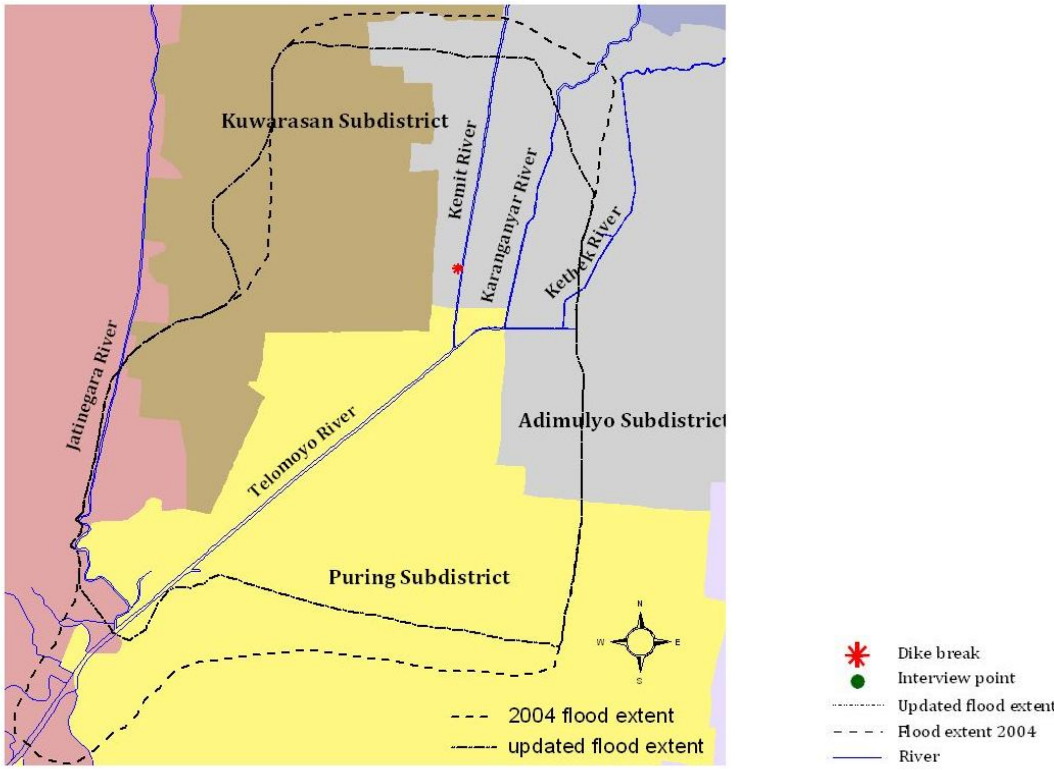

Figure 2-5. Existing flood extent map

3. Literature Review

3.1. Digital Elevation Model (DEM)

A Digital Elevation Model (DEM) is the representation of the terrain surface in which elevation points are stored as rectangular grid (Hunter & Goodchild, 1997). A single rectangular cell covers a certain area and is represented by one elevation value. There are several other digital formats to represent the DEM such as gridded format, a triangular irregular network (TIN), and contour lines (Wechsler, 2003). The gridded format DEM is more preferable since it can be easily stored and manipulated (Raaflaub & Collins, 2006). Among these three formats, the gridded DEM is the most commonly used in the environmental modeling due to its storage efficiency.

Many data sources have been applied to generate a DEM and performed vary vertical accuracy such as 1) ground survey with 0.06 m vertical accuracy (Desmet, 1997); 2) topographical map information e.g. elevation point, contour lines with half meter accuracy (Ardiansyah & Yokoyama, 2002); 3) stereoscopic (3D) images of aerial photographs or satellite imageries (ASTER, SPOT, Ikonos) which is ranging from 5 meters – 30 meters accuracy; 4) airborne laser scanning, LIDAR (Liu, 2008) may perform 15 cm accuracy; and 5) interferometry RADAR with 2 – 4 meters accuracy (Crosetto, 2002). Table 3-1 summarize the DEM vertical accuracy form various data sources. However, the objectives and level of research define which sources to be properly used.

Table 3-1. Summary of DEM vertical accuracy produced from various data sources

Data source	Coverage area	DEM resolution	Vertical Accuracy (m)
Ground survey	3.5 Ha	1 m	0.06
Topo map i.e. contour lines 1 : 25000, ci = 10 m	7.5 x 5 min quadrangle	10 m	0.19
Aerial Photos	671 km^2		0.5 m
ASTER-GDEM		15 m	20 – 30
IKONOS			6.5 m
SPOT 5	120 km x 60 km	5 m	5.1 m (in the field)
Airborne laser scanning			0.15 m
Interferometry RADAR	25 km x 35 km		2 – 4 m

3.1.1. DEM for Flood Modeling

A DEM can give an improved understanding of any information for geomorphic, hydrologic, climatic, and biologic studies. DEM plays an important role in environmental modeling due to the topography which controls the function of natural ecosystem (Chaplot *et al*., 2006). In case of hydraulic modeling, the topography is the most important factor describing the river channels and floodplains which can influence both flood hydraulics and areal extent of the simulated flood (Casas *et al*., 2006; Horritt & Bates, 2001)

There are two ways to represent DEM in flood modeling, TIN or regular grid. Advantage and disadvantage are attached to each DEM representation. Bonham and Carter (1996) explain that gridded DEM is not appropriate to be applied in large-scale flood modeling due to poor definition of areas with sharp relief changes. TIN format is able to give better representation of the channel geometry and it is adjustable with the additional data such as points of maximum heights, depression or break slope, or elevated features which can influence the hydraulic behavior of the river (Bates *et al*., 1996). Selecting the proper format of DEM for the flood modeling should consider the coverage of area and the accurate that should be achieved. In addition to that, the effect of spatial resolution on raster-based flood model should be considered. However, mesh resolution is the key parameter in hydrodynamic modeling since it defines the smallest features that are represented in DEM and time computation (Casas, 2006). Time computation is important issue in such modeling since it affects the model stability.

3.1.2. Geostatistical Interpolation

Once the elevation data has been collected, a DEM can be produced by using spatial interpolation methods. Spatial interpolation is a method to predict the value at a unvisited location based on values at visited locations within the same area. Li and Heap (2008) reviewed many interpolation methods that were used by environmental scientists. They categorized spatial interpolation into three groups: 1) non-geostatistical methods, 2) geostatistical methods, and 3) combined methods. This grouping is based on the amount of statistical analysis involved in the interpolation. Less statistical analysis is used in the non-geostatistical method. This method does not need a strict assumption about the spatial variability of the data (Hengl, 2007) or no secondary information of the variables needed (Li & Heap, 2008). As this spatial interpolation method is beyond of the scope of this study, thus this is not going to be discussed any further. Detailed explanation can be seen in Li and Heap (2008). Several non-geostatistical methods are listed below.

- Nearest neighbors
- Triangular irregular network (TIN)
- Natural neighbors
- Inverse distance weighting (IDW)
- Regression models
- Trend surface analysis
- Splines and local trend surface
- Thin plate splines
- Classification
- Regression tree
- Fourier series
- Lapse rate

In many studies, geostatistical method is considered as Kriging. "*Kriging is a generic name for a family of generalized least-squares regression algorithm, used in recognition of the pioneering work of Daniel Krige (1951)*" (Li & Heap, 2008). Kriging interpolation is able to provide an optimal interpolation with minimum variances. The spatial variation is used as the weight in the interpolation (Desmet, 1997). The theory of probabilistic are applied here and several statistical step need to be followed before a map generated (Hengl, 2007). Blomgren (1999) noted that interpolation of earth sciences data sets contains spatial continuity that has to incorporated in the interpolation. The spatial continuity can be represented by variogram. Thus, before doing the Kriging interpolation, variogram model should be conducted first. Variogram provides essential information for interpolation procedure such as sampling density, spatial pattern, and spatial simulation (Hartkamp, et al., 1999). The variogram is of the form:

$$\gamma(h) = \frac{1}{2}E(y(x) - y(x+h))^2 \quad (1)$$

where,

$\gamma(h)$	= semi-variogram, dependent on lag or distance h
$(x, x+h)$	= pair of points with distance vector h
$y(x)$	= regionalized variable y at point x
$y(x) - y(x+h)$	= difference of the variable at two points separated by h
E	= mathematical expectation

Variogram consists of three parameters i.e. nugget, sill, and range. *Nugget* expresses small-scale variability and sampling errors which may cause points to have different values although separated by small distances. *Sill* represents the variances of the data set within specific range. And *range* is the values where sill is reached. Range is the distance beyond which spatial continuity between points no longer exist (Blomgren, 1999). Figure 3-1 and 3-2 illustrate the parameters of variogram and four general variogram models, respectively. After a variogram is fitted, interpolation is now carried on. Three models of Kriging interpolation are described in the following sections by referring to Li and Heap (2008).

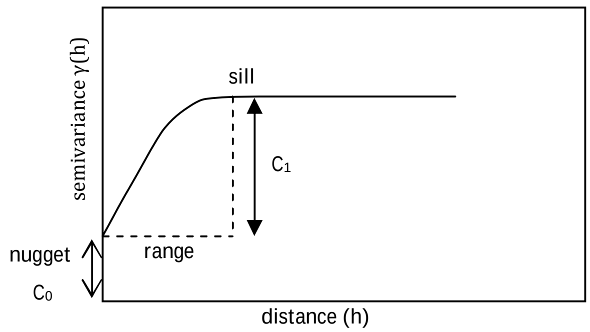

Figure 3-1. Variogram parameters

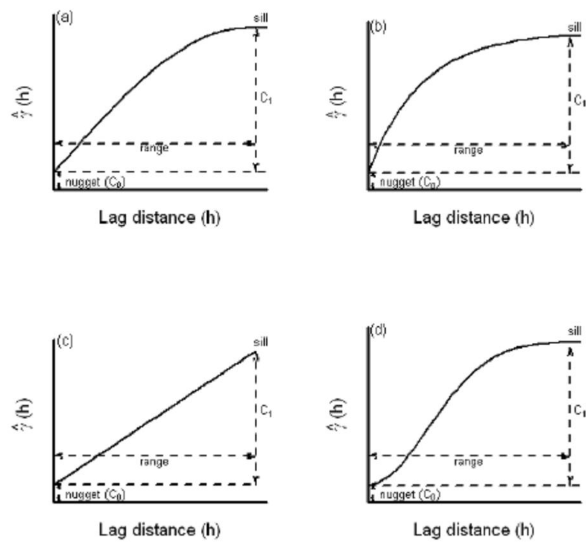

Figure 3-2. Variogram models taken from Li (2008) : (a) exponential, (b) spherical(c) linear, and (d) Gaussian

3.1.2.1. Ordinary Kriging (OK)

A standard version of Kriging interpolation is Ordinary Kriging (OK). The values at unsampled (grid) points are computed as a simple linear weighted average of neighbouring measured data point. The optimum weight is reached when the variogram is best fitted. The formula to compute ordinary kriging is taken from Hengl (2007). The model to predict the values through OK is as followed.

$$Z(s) = \mu + \varepsilon'(s) \qquad (2)$$

where μ is the constant stationary function (global mean) and $\boldsymbol{\varepsilon}'$(s) is the spatially correlated stochastic part of variation. The equation is developed into following equation

$$\hat{z}_{OK}(s0) = \sum_{i=1}^{n} \omega_i(s_0).z(si) = \lambda_0^T.z \qquad (3)$$

where λ_0 is the vector of kriging weights (ω_i), z is the vector of n observation at primary locations. According to de Smith (2006) ordinary kriging used point or block computation.

3.1.2.2. Simple Kriging

According to de Smith (2006), simple kriging assumes that the data have a known and constant mean value throughout the study area and exhibits the second order of stationary. The simple kriging is used when the data sets shows the trend (Bivand et al., 2008).

3.1.2.3. Regression Kriging

Identifying the structure of the data set before it is used is an essential step. Basically, Hengle (2007) explained the spatial structure could be identified by correlating the data sets with the environmental factors. Once the sampled variables and the environmental factor are correlated, the residual is investigated. If the residuals show the spatial auto-correlation then the regression kriging is allowed to be applied.

3.2. Description of DEM Error

"The DEM, as its name implies, is a model of the elevation surface. However, the DEM is often not treated as a model, but is accepted as a "true" representation of the earth's surface" (Wechsler, 1999).

Elevation model and other spatial data base are subject to error due to the imperfections in field measurement and the effect of topography generalization. A survey that aimed to find out the DEM user's perception on DEM uncertainty was conducted by Wechsler (2003). The result indicated that, 22% of the respondents believe that the uncertainty of the DEM is very important for any application. Thirty-three percent of the respondents perceive somewhat importance and 27% of the respondents never account the DEM uncertainty.

Fisher and Tate (2006) mentioned that errors in DEM can occur in both the elevation or vertical (Z) and planimetric or horizontal (XY) coordinates. The planimetric error may produce elevation error which is the so-called accuracy. Planimetric error deals with the accuracy of the GPS in determining the position. Uncorrected GPS coordinates may produce planimetric error when satellite imageries are being rectified (Gao, 2001). Fisher and Tate (2006) categorized the DEM error into three groups: *gross errors or blunders*, *systematic errors* due to deterministic bias in the data collection or processing, and *random errors*. Blunders are vertical errors associated with the data collection process, they are required to be identified and removed from the data. The systematic errors occur when the DEM is being interpolated and have fixed pattern, once the source is identified they should be eliminated. After removing the blunders and systematic errors, random errors still remain in the data due to the unknown of nature and location (Wechsler & Kroll, 2006). In general, the source of the DEM error can be categorized into two groups: *observation error* which depends on the way the elevation data are collected and *interpolation error* where the height between sampled points are estimated (Paquet, 2010).

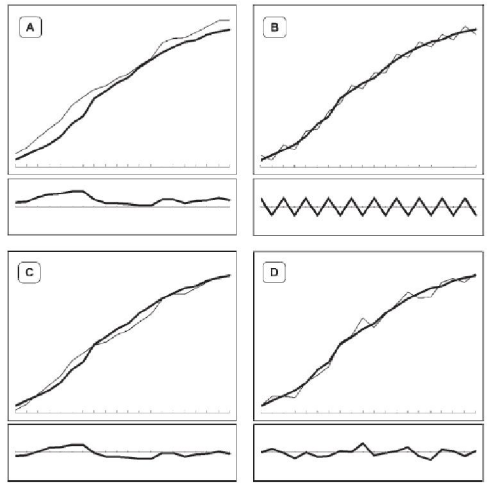

Figure 3-3. The comparison of DEM profile and the error occurrence. (A) bias error; (B) systematic error; (C) spatially auto-correlated error; (D) random error. The thick line represents the ground surface and the thin line represents ground surface with error, taken from Fisher (2006).

The information of DEM uncertainty only provides the global estimates of root mean square error (RMSE), the information about the accuracy at specific location within the DEM is not mentioned (Holmes *et al*., 2000). Hunter and Goodchild (1997) explain that the U.S. Geological Survey (USGS) assess their DEM product by comparing a minimum of twenty - eight test points (eight on the boundary and twenty inside the file) with ground control point (GCP) values taken as the true value. The accuracy of the DEM can be estimated using this following expression,

$$RMSE = \left[\sum_{i=1}^{n} \left(z_i - z^*_i \right)^2 / n \right]^{1/2} \tag{4}$$

where n is the number of sample points, i indicates the sampled point, z_i is the elevation of the DEM at the sampled point, and z^*_i is the true value at sampled point. It can be noted that the accuracy of the DEM is assessed by comparing the interpolated DEM with the reference value (Desmet, 1997).

The RMSE would be equal to the standard deviation if the mean error is zero or to be estimated as zero. Researchers suggest estimating the other statistical description such as mean error (ME) and standard deviation (S) in case of the mean error fall into zero (Fisher, 1998; Fisher & Tate, 2006).

$$ME = \left[\sum_{i=1}^{n} \left(z_i - z^*{}_i \right) / n \right] \quad (5)$$

$$S = \sqrt{\frac{\sum_{i=1}^{n} \left(z_i - \bar{z} \right)^2}{n}} \quad (6)$$

Uncertainty in the topography could be assessed by quantifying the systematic error. Wechsler (2006) explained that statistic measurement such as bias could be applied to quantify the systematic error. Bias measures the degree to which predicted parameters are, on average, above or below the true parameter at a cell location. The formula is presented below.

$$Bias = \frac{\sum_{i=1}^{N} (z^*{}_i - z_i)}{n} \quad (7)$$

3.4. Hydrodynamic Modeling

Hydrodynamic models are driven by tidal, discharge, wave, and meteorological forcing. These models are available in wide range of types, from simple 1D models to complex 2D models. In model, flow direction is important element which is needed to consider (Prachansri, 2007). Furthermore, 1D models are applied for studying flood levels and discharges in river system. For the open water flow, rainfall runoff model is considered in hydrodynamic modeling so that it is able to do hydrological routing.

3.4.1. 1D Flood Modeling

One dimensional model of river hydraulic is typically parameterized by a series of channel cross-section which perpendicular to the flow direction and floodplain topography. This cross-section can be obtained from ground survey at a reasonable cost. This model is best applied in the area with clear and well-defined valleys where the flow is clearly one-directional, in case the lateral spread happens instantaneously as the water level in the river rise. The approach of this model is based on the Saint Venant equation for unsteady open channel flow described by (Horrit & Bates, 2002).

$$\frac{\partial A}{\partial t} + \frac{\partial \emptyset Q}{\partial x_c} + \frac{\partial (1-\emptyset) Q}{\partial x_f} = 0 \quad (8)$$

$$\frac{\partial Q}{\partial t} + \frac{\partial}{\partial x_c}\left(\frac{\emptyset^2 Q^2}{A_c}\right) + \frac{\partial}{\partial x_f}\left(\frac{(1-\emptyset)^2 Q^2}{A_f}\right) + gA_c\left(\frac{\partial_z}{\partial x_c} + S_c\right) + gA_f\left(\frac{\partial_z}{\partial x_f} + S_f\right) = 0 \quad (9)$$

$$\emptyset = \frac{K_c}{K_c + K_f} \quad \text{where} \quad K = \frac{A^{5/3}}{nP^{2/3}} \quad (10)$$

$$S_c = \frac{\emptyset^2 Q^2 n_c^2}{R_c^{4/3} A_c^2} \qquad S_f = \frac{(1-\emptyset)^2 Q^2 n_f^2}{R_f^{4/3} A_f^2} \quad (11)$$

The equation above takes several parameters into account such as Q which represent the total flow down to the reach, A as the cross sectional area of the flow in channel (A_c) and floodplain (A_f), x_c and x_f are distances along the channel and floodplain, respectively, P as wetted perimeter, R as hydraulic radius (A/P), n as Manning roughness value, and S as the friction slope. The channel and floodplain flow is separated by ϕ according to the conveyances K_c and K_f. Bates (2000) mentions the flood extent simulation in 1D depends on the water depth value at each cross section. The flood extent in floodplain or at each cross section is identified by linear interpolation. Main limitation is that floodplain inundation is badly represented, especially for dike break scenarios.

3.4.2. 2D Flood Modeling

Two dimensional models have been developed in more detailed way for simulating distributed patterns of floodwater flow depth and depth-averaged velocity, to investigate the hydraulic characteristic of natural floodplains. These models consider flow direction in both horizontal directions, allowing calculation of more detailed water levels along the river to get better prediction of flooding. 2D hydrodynamic model gives insight into the development of the inundation that results from a breach in the flood defense (Jonkman *et al*., 2008).

Once the terrain become more complex such as flood plain, the 1D model should be shifted into 2D model. The 2D model requires continuous representation of the terrain topography in form of digital surface model (Alkema, 2007).

3.4.3. 1D2D Flood Modeling in SOBEK

SOBEK Overland Flow formerly known as Delft-FLS model, developed by DELTARES, is able to to integrate The Overland Flow (2D) and 1D flow model. The overland flow model (2D) module in SOBEK-Rural is designed for the calculation of two-dimensional flooding scenarios. To obtain the accurate flood modeling, 1-dimensional river flow module is integrated (SOBEK help). This model is based on two-dimensional solution of the Saint Venant equation which is derived from 3D incompressible equation of Navier-Stokes by depth-averaging the mass continuity and momentum balances (Alkema, 2007). Such equation solves the non-steady free surface flow in shallow water environment. The calculation of water depth and depth averaged velocity is at each grid at each time step (Frank et al., 2007).

3.5. Flood Hazard

3.5.1. Definition of Flood Hazard

Hazard is defined as a potentially damaging physical event, phenomenon or human activity that may cause the loss of life or injury, property damage, social and economic disruption or environmental degradation. Hazards can include latent conditions that may represent future threats and can have different origins: natural (geological, hydrometeorological and biological) or induced by human processes (environmental degradation and technological hazards). Hazards can be single, sequential or combined in their origin and effects. Each hazard is characterized by its location, intensity, frequency and probability (ISDR, 2004). Flood hazard is defined as the chance of a certain magnitude of flood event to occur in a given area and period of time (Alkema and van Westen, 2005).

Flooding is a natural and recurring event for a river or stream. Flooding is a natural process which can both be advantage to the societies or cause damage. However, population growth leads to population pressure. Economic activities drive infrastructure development near to the rivers, as the number and susceptibility of settlement increase, the flood hazard remains the same but the flood risk becomes higher.

4. Digital Elevation Model (DEM)

4.1. Overall Methodology

This chapter covers three main steps, 1) DEM generation based on point data, 2) adjusting the DEM with the elevated features for hydrodynamic modeling, and 3) adding the noise to study the error propagation of the DEM error in hydrodynamic model. Figure 4-1 represents the detailed workflow of the DEM generation process. A set of 18827 elevation points from SJFCSP was first explored to identify the basic statistical parameters and the presence of surface trends. The information produced in the first stage was then used to develop the variogram model before point interpolation carried on. The point interpolation in the second stage was conducted through three methods i.e. Simple Kriging, Ordinary Kriging, and Regression Kriging. The uncertainty of the prediction was also analyzed in this stage. The accuracy of generated DEMs was assessed in the third stage. The standard deviation, RMSE, and bias were chosen to calculate the DEM's accuracy. The last stage was the DEM adjustment with the built-up area.

4.2. Exploratory Data Analysis

4.2.1. Data Distribution

The original elevation points cover wide flat terrain and narrow steep hilly terrain in the southern part (Karang Bolong Hills). The elevation of the hilly terrain is ranging from 20 m to 50 m above mean sea level. This condition affects the distribution of the elevation points which are shown by Figure 4-2a. The original data is very right skewed indicated by the long tail. To get closer to a normal distribution, 40 points in the hilly terrain were removed. The point removal was not only based on the data normality requirement for standard statistical analysis, but also the focus of the study. Removing the points in the hilly area did not significantly the distribution of the data since the right-skewed data remained present. The effect of point removal was the decreasing of the standard deviation from 3.176 m to 2.968 m (see Table 4-1).

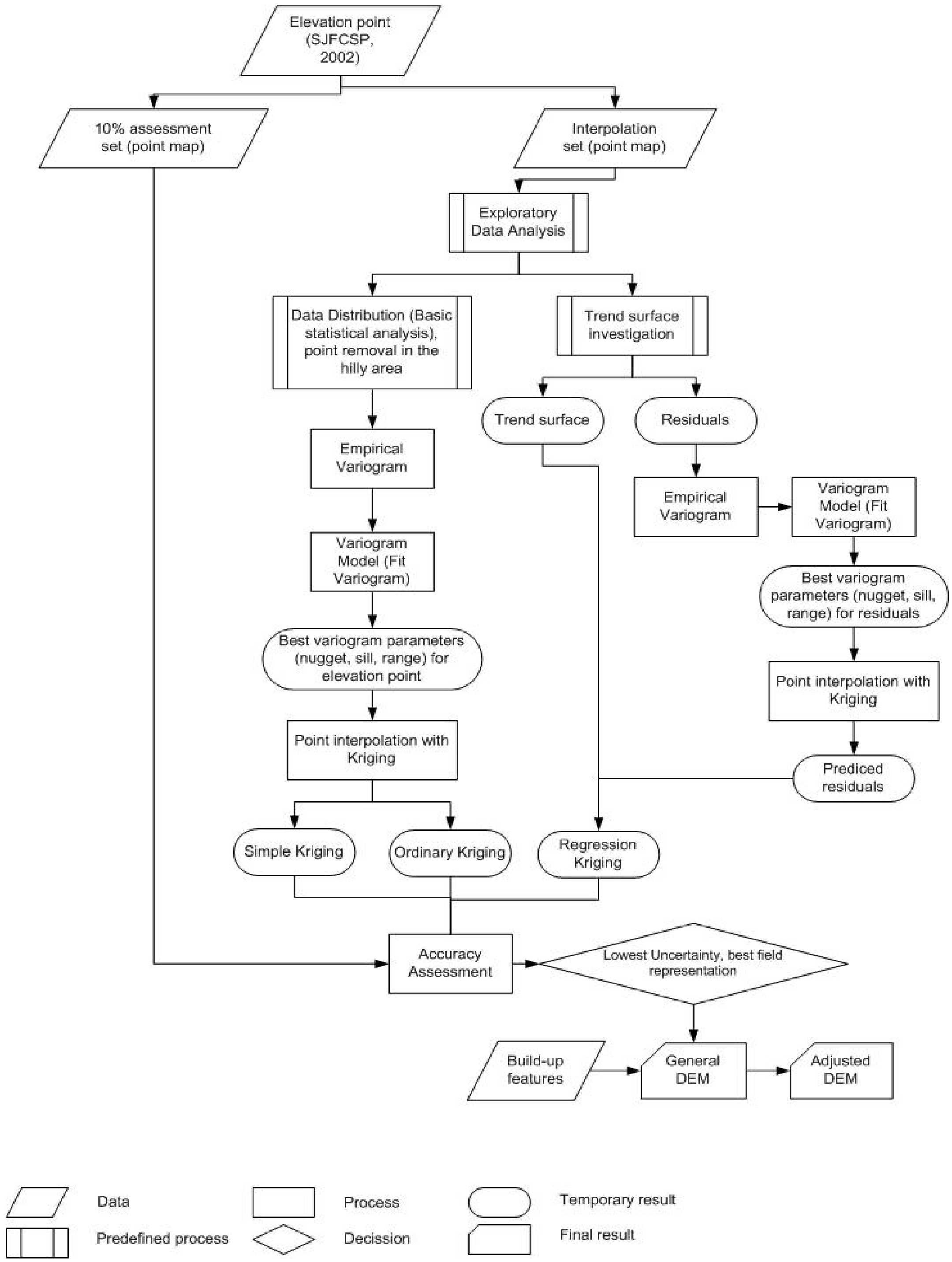

Figure 4-1. The workflow of DEM generation

For the accuracy assessment, 10% of the points in the floodplain area were selected and stored as independent point. These independent points were used in the accuracy assessment in the stage 4. The rest of 16909 elevation points were used to generate the DEM through interpolation technique. By removing another number of points the standard deviation was slightly decreasing by 6 mm (see Table 4-1). Spatial distribution of the elevation point is shown in Figure 4-2. Most of the elevation points in the flat terrain fall on 3 to 8 meters above mean sea level and these points fit in the normality line (see Figure 4-3). The overall elevation point was higher than the standard value in the normality line. Data transformation is not necessarily conducted since this study did not need normal distribution as the other models do.

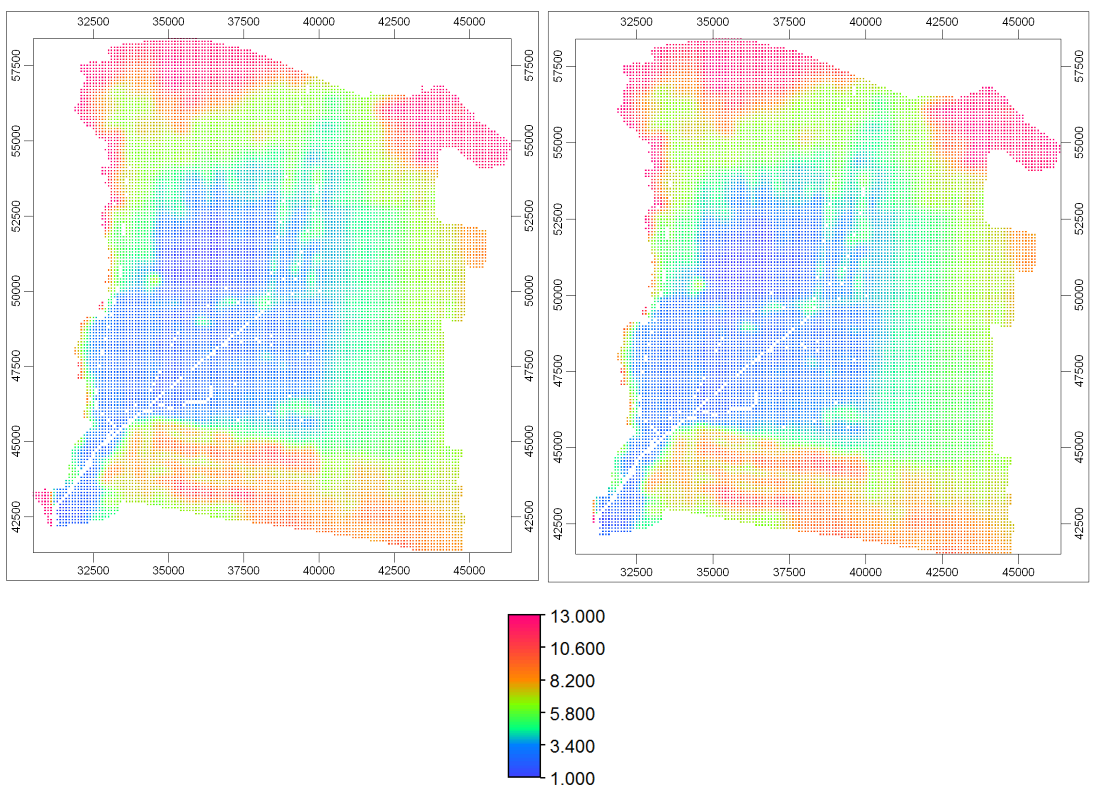

Figure 4-2. The spatial distribution of elevation point for initial data (left) and after the hilly area removed (right)

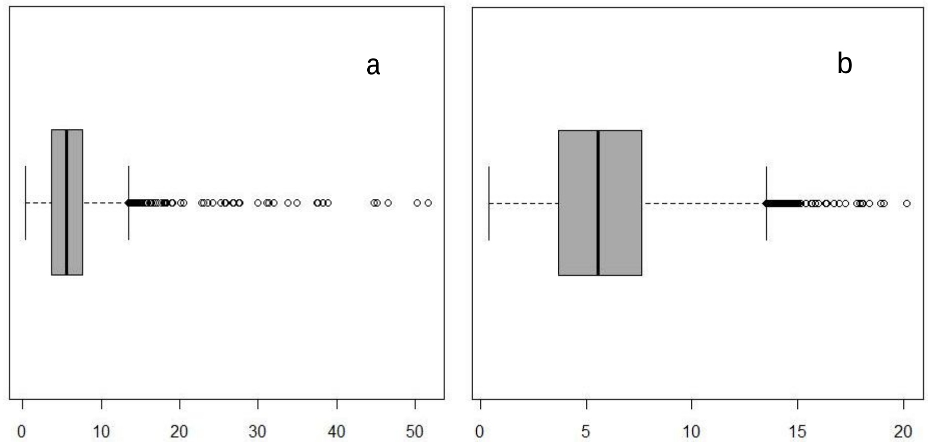

Figure 4-3. Boxplot of the elevation point (a) original point (b) hill removed

Table 4-1. Statistic summary of elevation points

Statistical information	Original point	Hill removed	Interpolation point set	Assessment point set
Number of points	18827	18787	16909	1878
Mean (m)	5.94	5.94	5.93	6.01
Median (m)	5.58	5.57	5.56	5.38
Std. deviation (m)	3.18	2.97	2.96	3.02

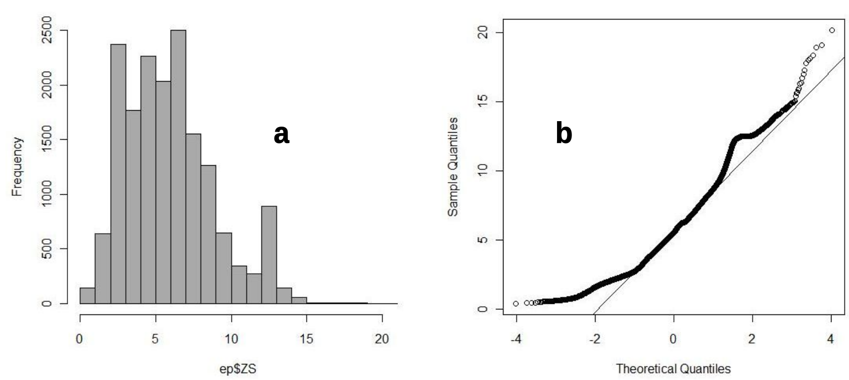

Figure 4-4. Data distribution of interpolation point (a) histogram (b) Quantile-Quantile plot

4.2.2. Trend Surface Investigation

The investigation of the trend surface needs to be conducted to describe the global variation of elevation over the study area. The trend surface tells about the dependency of the elevation on its location (coordinates). The correlation of the elevation and the coordinates of the data were identified through linear model. The trend surface removes the spatial variability, thus it is needed to investigate.

The first order of trend surface showed that the elevation of the study area is constantly changing from NE to SW (Figure 4-4). Each kilometer south the elevation increases by 0.18 mm. The model is able to explain only 10.07% of the variation indicating by the R^2 (see Table 4-3) with the residual standard error 2.81 m. The coefficient indicates that the variation of the elevation is not significant as the changing of the coordinates. Since the study area is dominated by flat areas thus the coefficient is logical. The coefficient is less than 0.5 meter meaning that the area tends to be more homogeneous. The residual in Figure 4-5 performs the structured pattern. The lowest residuals (red color) are located in the center of the study area where the edge of the study area shows positive residuals (green color). The elevation of beach ridges in the southern part was overestimated indicating by the positive residuals. The northern part of the study area agrees with this situation. The variation of the elevation in undulating and inclined area was abrupt thus overestimate the prediction.

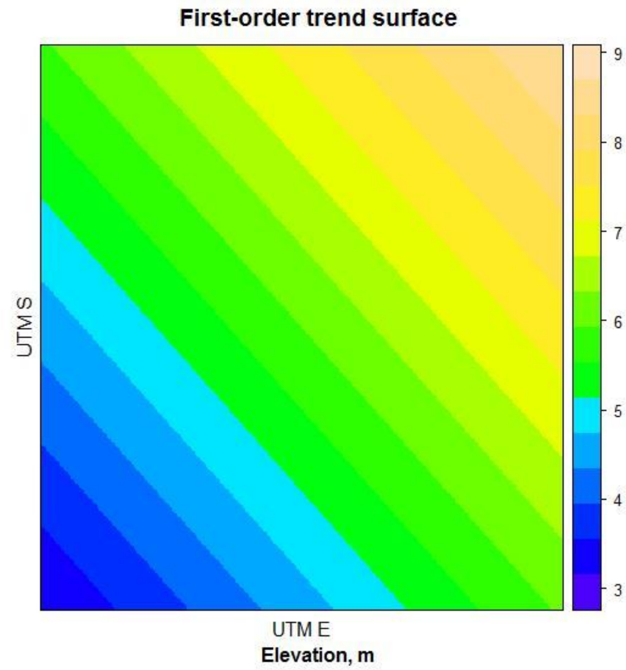

Figure 4-5. 1st order trend surface model, elevation is shown in meter

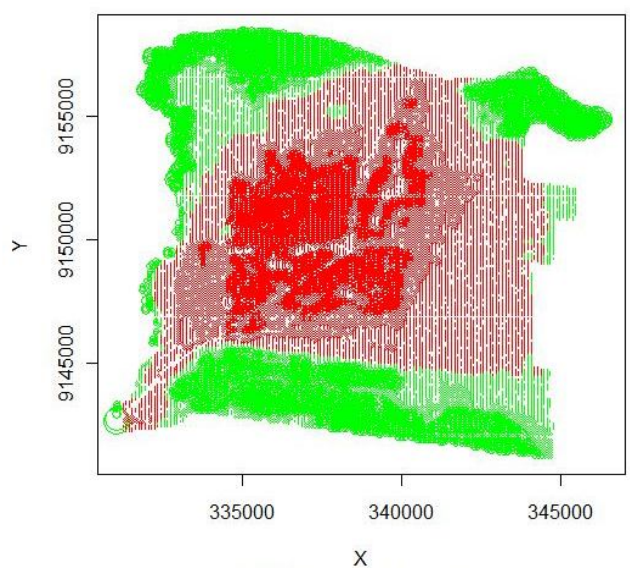

Figure 4-6. Residuals points of 1st trend surface indicating the difference between modeled and observed values. Green means positive differences (overestimate) and red means negative differences (underestimate)

Table 4-2. Summary of the 1st order trend surface model

Trend surface parameters		Values (m)
Residuals	Min (m)	-5.27
	Median (m)	-0.72
	Max (m)	16.68
	Std. error (m)	2.81
Model estimation		Elevation = -1506 + 0.00018(X) + 0.00016(Y)
Adjusted R-squared (%)		10.07

The second order trend surface was performed to get the better fit of the model to the reality. This higher order of trend surface explained the variability better than the first order did. The R^2 of the model was 65.12% with the residual standard error 1.75 meter (see Table 4-3). The trend surface exhibited the parabolic pattern. The equation used in the second order trend surface contained the linear and quadratic model. It then produced bowl shape pattern. The lowest part is still in the center of the study area. The northern and southern part was represented by high elevation point (see Figure 4.6). Residual of the second order trend surface was less structured than that of the first order (Figure 4-7). Positive residuals were still located in the beach ridge and in the foot slope of the Karang Bolong Hill, in the western part of the study area. The model overestimates in the hilly area and underestimates in the lowland area. Since the 2nd order trend surface performs better model, it was then used for further analysis.

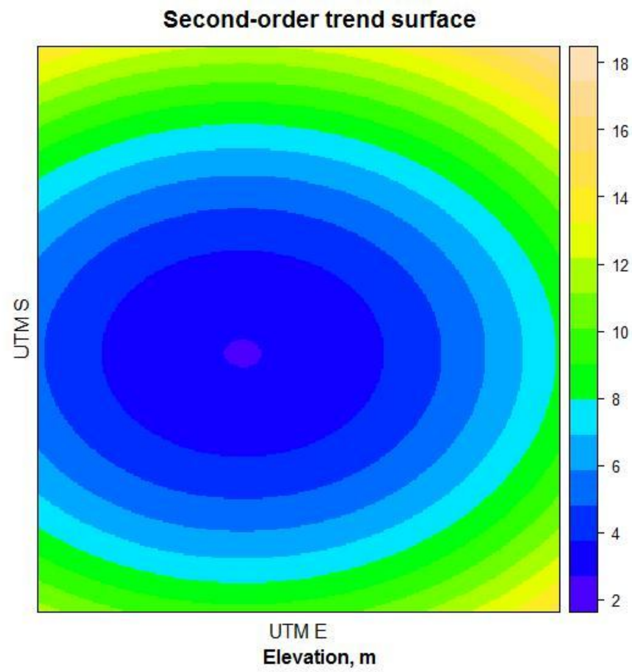

Figure 4-7. **2nd** order trend surface model, elevation is shown in meter

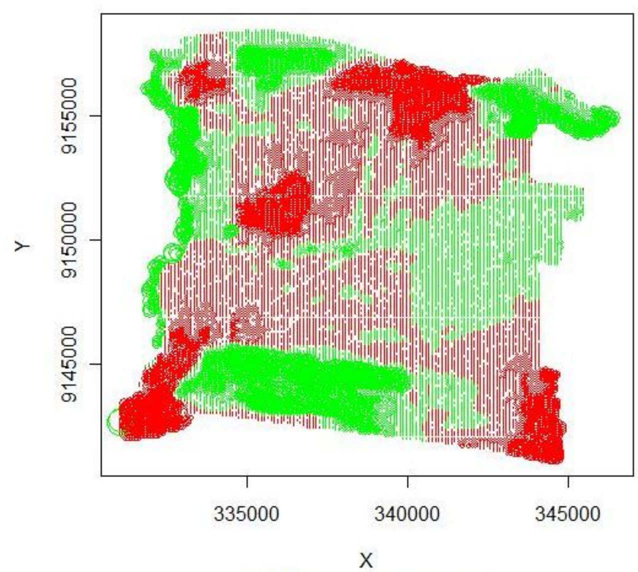

Figure 4-8. Residuals points of 2nd order trend surface indicating the difference between modeled and observed values. Green means positive differences (overestimate) and red means negative differences (underestimate)

Table 4-3. Summary of 2nd order trend surface model

Trend surface parameters		Values
Residuals	Min (m)	-7.74
	Median (m)	-0.16
	Max (m)	11.09
	Std. error (m)	1.75
Model estimation		Elevation = 9.10e+06 + 5.81e-08$(X)^2$ -0.04(X) + 1.09e-07$(Y)^2$ -1.99(Y)
Adjusted R-squared (%)		65.12

4.3. DEM interpolation and Associated Uncertainty

4.3.1. Variogram

In the previous section 4.2.2, the strong spatial structure was identified. The elevation point is considered as the continuous data in which the spatial continuity exhibits. Blomgren (1999) noted that spatial continuity means that the closer points are more likely to have similar value than two points separated by greater distance. The spatial continuity is approached by developing the variogram to perform the variance between the values. The variance is based on the distance between the points.

The empirical variogram of the elevation point was conducted with descending cutoffs, from larger to shorter. The spatial variability in the low land area only can be investigated trough the shorter range. Figure 4-8a shows the spatial continuity within range of 15000 meters. Larger cutoff allowed the higher variance to perform up to 3.464 meters ($\sqrt{12}$ meters). After the distance of 10000 meters the variance decreased and started to increase at 13000 meters. This variance change within relatively short range explained the presence of the beach ridges in the southern part. The presence of the beach ridges in the study area performed the nugget value which was around 1 meter. Since this study was focusing in the flat terrain, the variance in the beach ridges was ignored.

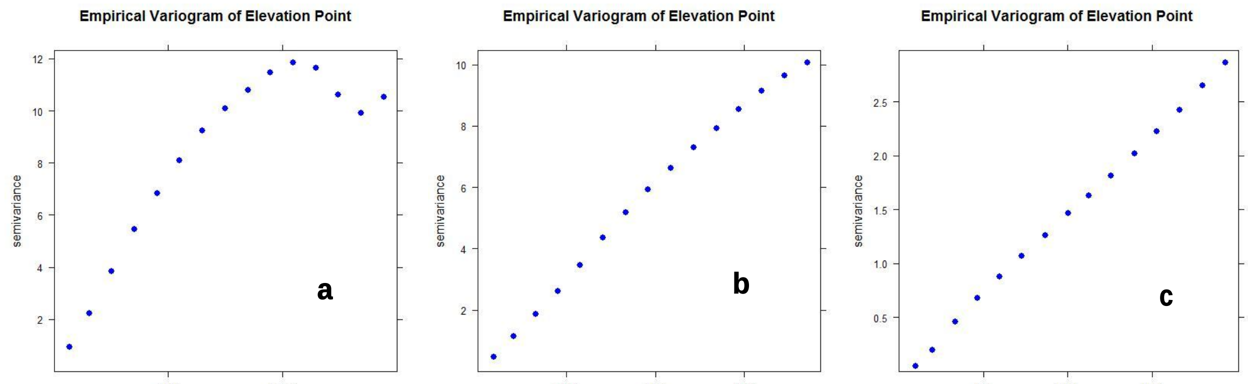

Figure 4-9. The empirical variograms of elevation point with descending cut offs, (a) 15000 meters (b) 6000 meters and (c) 2000 meters

The analysis proceeded to shorter range, 6000 meters. The aim of using shorter cutoff was to get more detailed point structures. The elevation values were well structured due to the absence of abrupt changes in terrain. Within this range, the variance reached up to square root of 10 meters or 3.16 meters (see Figure 4-8b). The shortest cutoff performed in this stage was 2000 meters. The similar continuity was found within this range but closer points separated by 200 meters did exhibit low variances at the beginning. Ignoring the beach ridges has decreased the nugget effect to 0.2 meter in 6000 meters cutoff and 0.1 meter in 2000 meters cutoff. The presence of the nugget effect might be affected by the error when the measurement conducted.

Once the empirical variogram was created, the fitting of the variogram was conducted. The fitting of the variogram is a trial and error process to get the best model and parameters. After several attempts, the 6000 meters cutoff variogram was chosen to be basis of the fitting variogram. Very large range performed high variance and smoothed the interpolation. Very short range limited the point pairs thus there was no adequate point density to be interpolated.

The fitted model by eye take these parameters, 0,2 meter nugget, 14 meter sill, and 6500 meters range. The effective range of exponential model is three times the range parameters of the variogram model. In this study, the effective range was 14535 meters

(95% of the study area extent), thus the range parameters was supposed to be 4845 meters. A range parameter adjustment was taken to obtain the best fit. The model fit by eye was compared to gstat's package in R by taking the least square fit. The model fit by eye was close to the automatic fit model (see Figure 4-9). Hence this variogram fit was used for the interpolation technique.

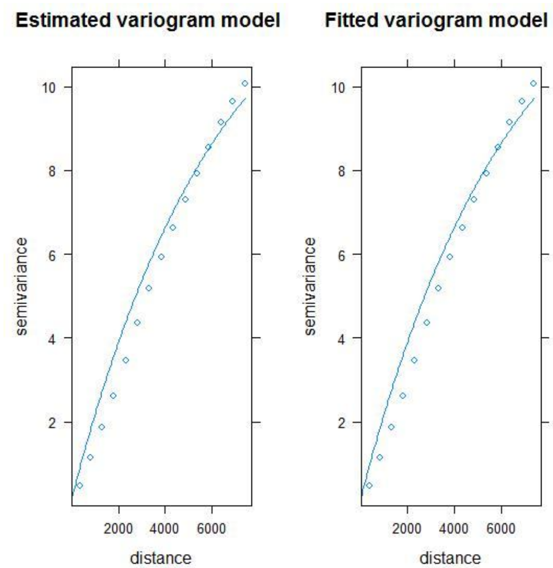

Figure 4-10. Varioram fitting based on eye observation and gstat's automatic fitting model

4.3.2. Kriging Interpolation

The available elevation point was in the form of point data with 100 meter spacing, In order to get the continuous elevation data, thus interpolation is needed. In this study, three interpolation methods were applied to predict the elevation. The methods were Simple Kriging, Ordinary Kriging, and Regression Kriging. In order to define which method is the proper one, the decision tree in Figure 4-11 was used. Based on the decision tree, the simple kriging was the most proper. However, two ather methods of kriging were also applied to compare the result. The simple kriging and ordinary kriging were used to predict the elevation value by using the elevation data itself as single predictor. The simple kriging and ordinary kriging have the similar assumption of which the mean are constant in the study area. The regression kriging is used to interpolate the residual which then to be added to the trend surface. This was aimed to add the local structure to the trend.

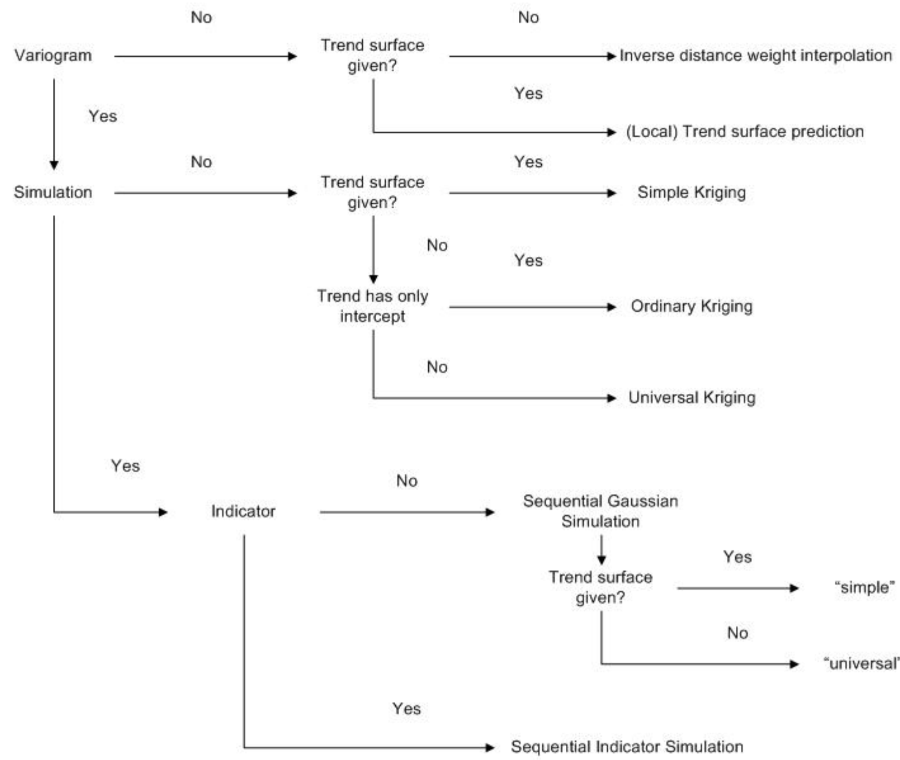

Figure 4-11. Decision tree for kriging interpolation (Bivand, 2008)

These three methods gave varying values of the interpolated DEM. The values were summarized in Table 4-5. The simple kriging interpolation resulted the least values among the others. Figure 4-12 shows the interpolated DEM produced by Simple Kriging and Ordinary Kriging. The interpolated DEM by using simple kriging or ordinary kriging did not show significant difference. The simple kriging tend to have small value at the boundary of the study area. The variance of the prediction is greater when no data available outside the study area.

Table 4-3. Summary of DEM interpolation using three methods of kriging

Methods	Minimum (m)	Maximum (m)	Mean (m)	Median (m)
Simple Kriging	0.00	20.87	4.74	4.65
Ordinary Kriging	0.44	21.27	6.17	5.89
Regression Kriging	0.44	26.17	6.83	6.42

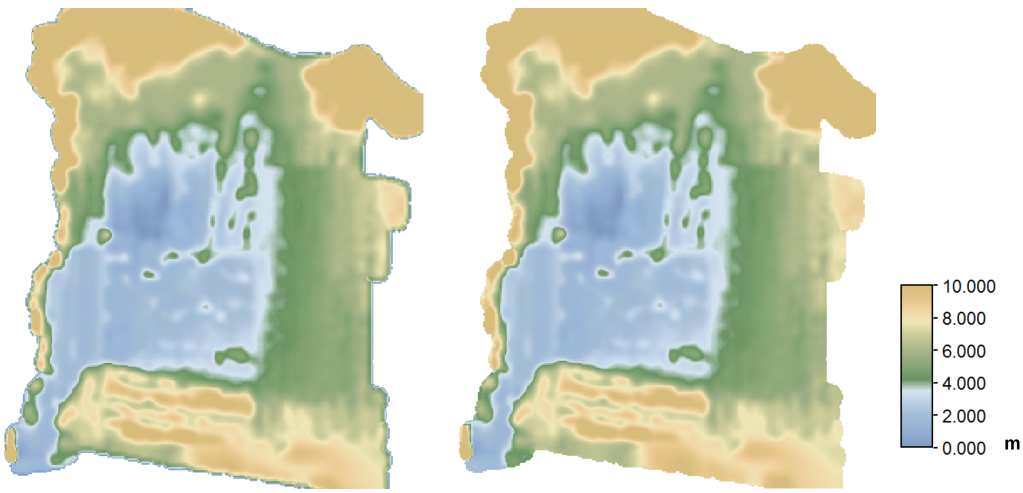

Figure 4-12. Predicted elevation in meter based on simple kriging (a) and ordinary kriging (b).

The regression kriing was done by adding the predicted residuals to the trend surface. The predicted residuals were the local variation. This was aimed to remove the global trend of the data set. Figure 4-13 shows high residuals produced the high elevation values.

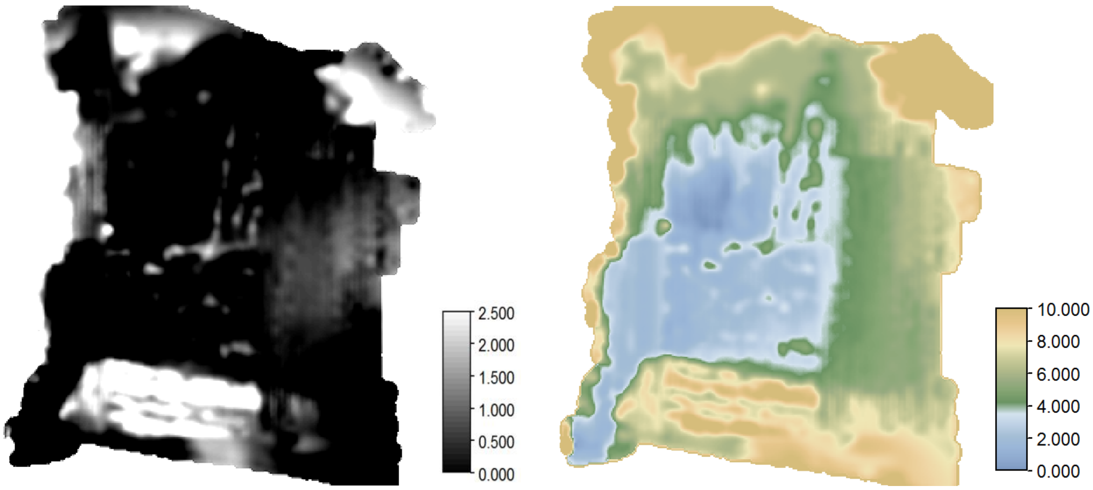

Figure 4-13. The predicted elevation values from regression kriging, in meter. The prediction (right) was resulted from residuals and trend surface

4.4. DEM Accuracy Assessment

The interpolated DEMs were then compared to the independent points. Figure 4-14 showed the spatial distribution of the independent points. Standard deviation, bias, and root mean square error were chosen to assess the error of the interpolated DEM. The random error of the interpolated DEM was reflected in the standard deviation. Systematic error of the interpolated DEM was quantified by the bias. The last accuracy assessment was based on the RMSE which incorporates both DEM error type. Table 4-5 summarizes the vertical accuracy of the three interpolated DEMs. The interpolated DEMs performed the similar number of the standard deviation and the RMSE. The significant difference was found in bias in which the Regression Kriging showed greater bias -0.04. The negative value indicated that the interpolation was underestimated or the predicted values were less than the observed values.

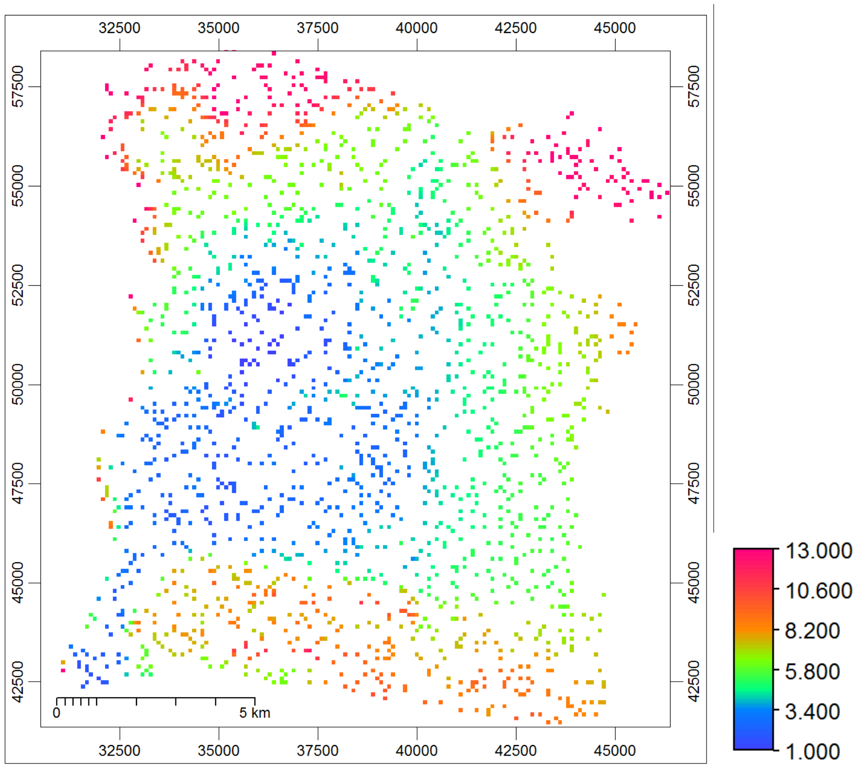

Figure 4-14. The spatial distribution of the independent points used for accuracy assessment

Table 4-4. Summary of the prediction error of DEM

Kriging	Standard deviation (m)	Bias (mm)	RMSE (m)
Simple Kriging	2.98	-0.01	0.31
Ordinary Kriging	3.00	-0.01	0.32
Regression Kriging	3.03	-0.04	0.31

4.5. Built-up features

The DEM was adjusted by existing built-up features such as railways, road, and river dike. The elevated feature was added into the elevation model.

1) Roads and railways

   Roads and railways network were extracted from the topographic map and used for the basis of the measurement point. Several point measurements were done to obtain the thickness of the road asphalt and the elevated railways. Figure 4-15 illustrates the road network which is classified into national road, local road, and unclassified. The average of the road asphalt thickness was 3.46 cm and the railways were elevated up to 137.5 cm.

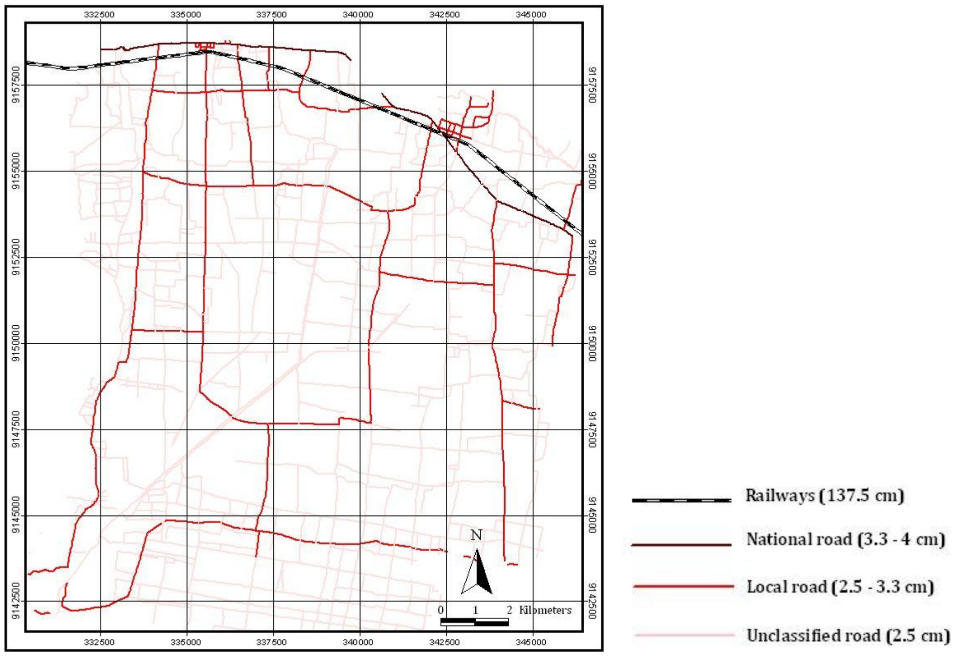

Figure 4-15. Road network and railways added to DEM

2) River dike

River dikes have been essentially protection infrastructure in the study area. The height of the dike is necessary to be identified due to its effect on the flood propagation. The height was extracted from as built drawing which was conducted by SJFCSP. The height extraction was carried out by manual digitizing in vector form and rasterizing afterward. Detailed dike height is illustrated in Figure 4-16.

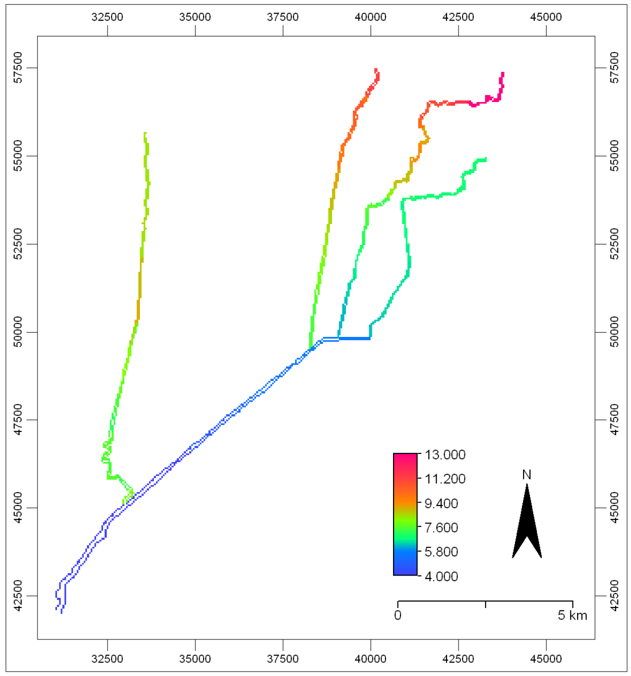

Figure 4-16. Extracted dike height

5. Hydrodynamic Modeling

5.1. Methodology

The flood modeling in this study was carried out in 1D2D model in SOBEK. This type of model combines the water flow in channel (1D) and the overland flow on the terrain (2D). The flood modeling was conducted based on four different return periods. The hydrodynamic modeling was aimed to provide the map of depth of inundation and maximum velocity. The model was calibrated by using historical past event data. Figure 5-1 illustrates the detail workflow of the flood modeling.

The 1D modeling requires river cross sections to represent the river channel. While the 2D modeling needs DEM to represent the terrain. In this study 50 meter DEM resolution was used. The coverage and homogeneity of the area were the basic consideration in selecting the DEM resolution. For the detailed flood modeling, such DEM resolution is very coarse to represent the micro topography of the terrain for example small depression. Thus, the detailed river cross sections were used in the 1D modeling. The flood simulation was carried for the 2yr, 5yr, 10yr, and 25yr return periods. The model calibration was done by changing the surface and channel roughness. Due to the limitation of the available data, the calibration was done only for 25yr flood model.

5.2. Input Data

5.2.1. Flood Hydrograph

For the 1D channel flow model, hydrological condition is required in setting up the upstream boundary condition. SOBEK provides several options such as water level (constant, tabulated function time) and discharge (constant, tabulated function of time, tabulated function of the water level). In this study, a flood hydrograph was selected as the relation of flood discharge and time in the upstream boundary. This flood hydrograph was derived from the rainfall-runoff model which was modeled by BCEOM consultant for SJFCSP. The rainfall was designed for the different return period through the frequency analysis. The peak discharge was calculated by using Snyder's Synthetic Hydrograph. The duration of the 2004 flood was approximately 72 hours, thus the flood hydrograph was linear extrapolated (Figure 5-2 to 5-5). The summary of the designed rainfall and peak discharge is shown in Table 5-1.

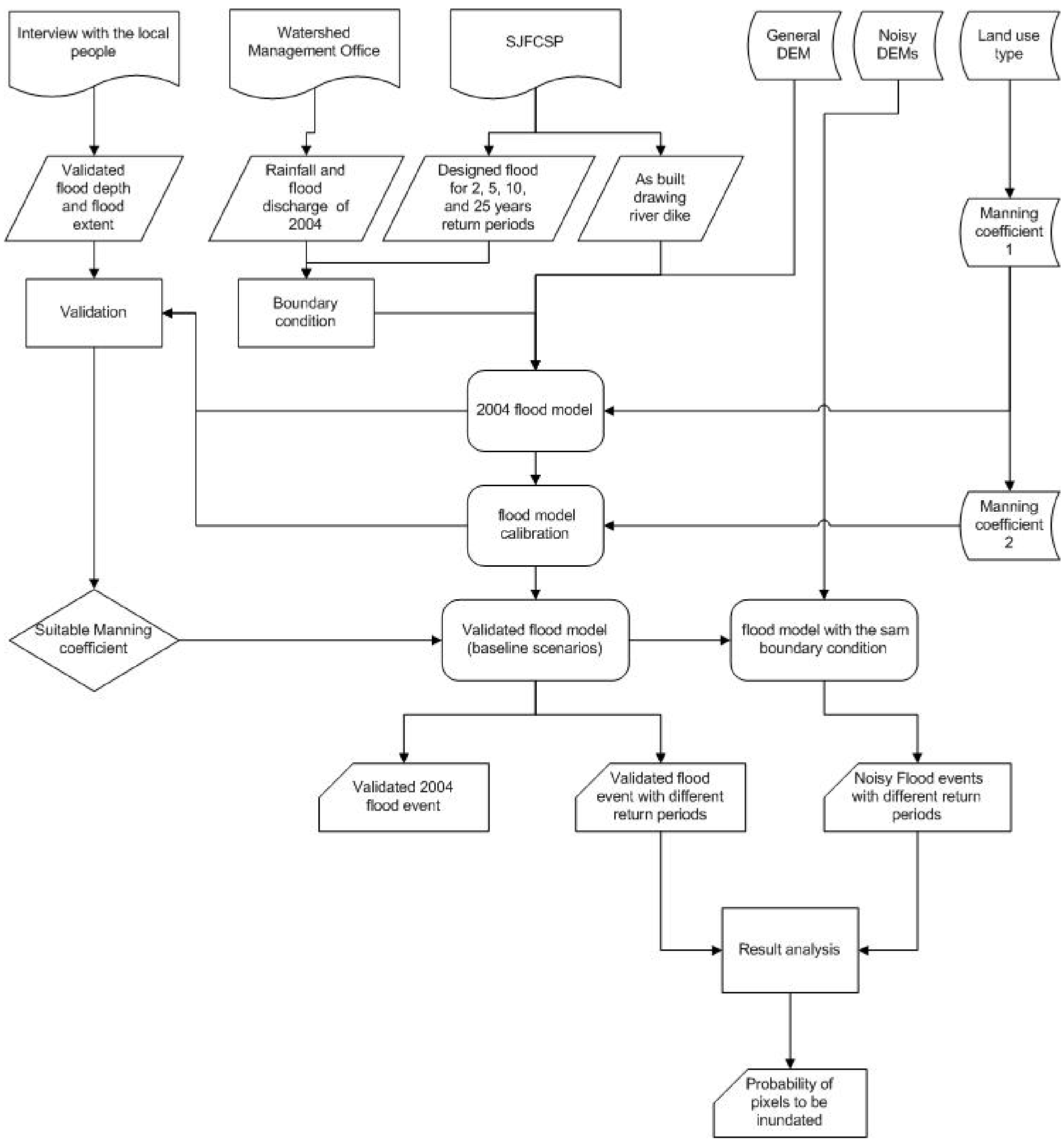

Figure 5-1. The workflow of flood modeling

Table 5-1. Summary of designed rainfall and peak flow of the study area used by SJFCSP (BCEOM, 2003)

Sub Catchment	Return Period		
	Years	**Rainfall (mm)**	**Peak Flow (m^3/s)**
Kemit	2	133	128.92
	5	175	198.39
	10	200	244.53
	25	251	313.26
Karanganyar	2	134	76.58
	5	172	96.62
	10	198	126.07
	25	243	141.96
Ketek	2	134	68.83
	5	172	86.21
	10	198	93.24
	25	243	102.78
Jatinegara	2	135	113.62
	5	181	149.11
	10	210	167.88
	25	274	199.77

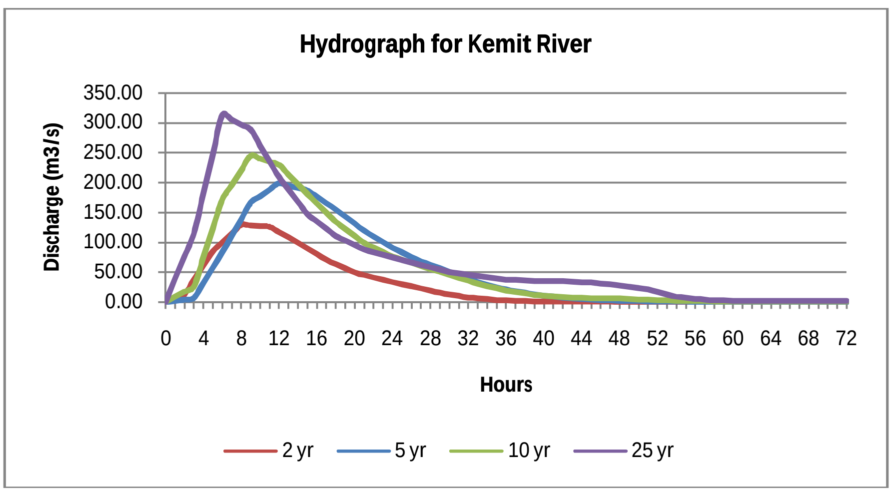

Figure 5-2. Extrapolated flood discharge of Kemit River

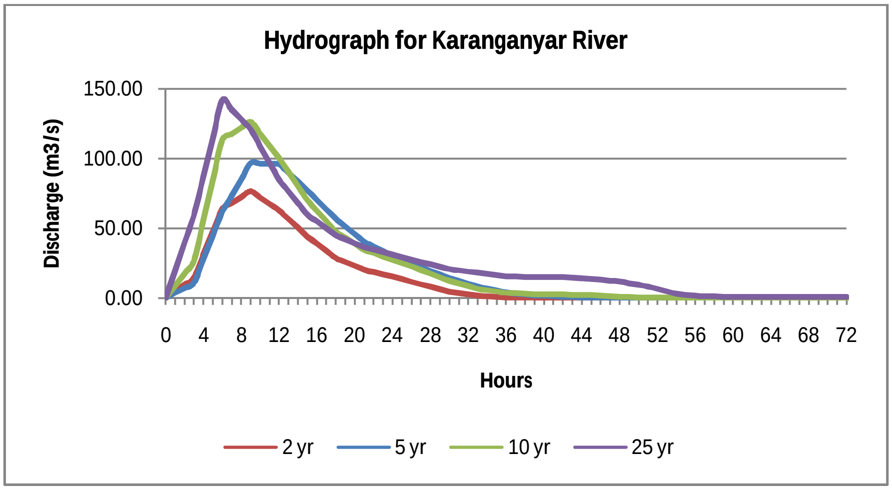

Figure 5-3. Extrapolated flood discharge of Karanganyar River

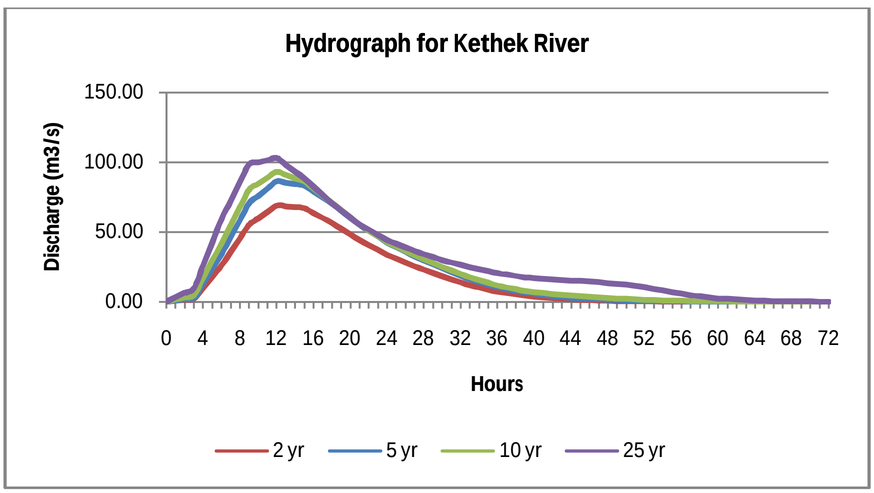

Figure 5-4. Extrapolated flood discharge of Ketek River

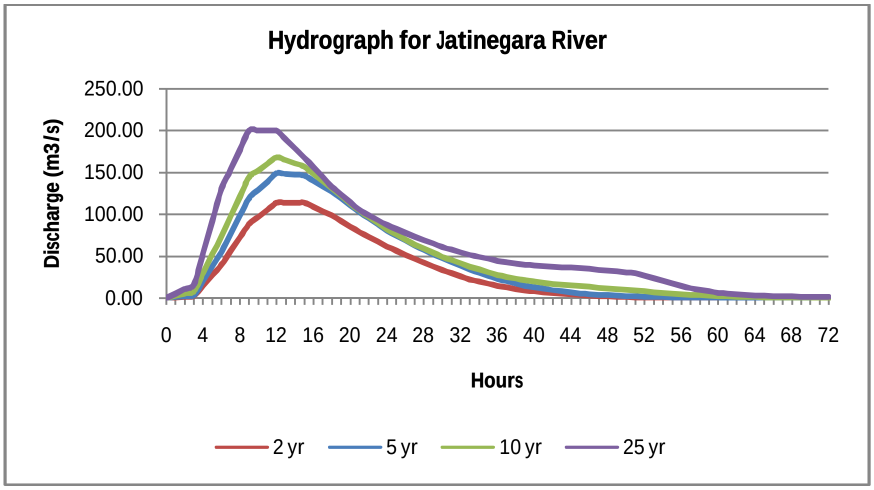

Figure 5-5. Extrapolated flood discharge of Jatinegara River

5.2.2. Cross Sections

An essential element of flood modeling in SOBEK is river cross section. A cross section represents the shape and size of the river which is perpendicular to the river. In this study, the cross sections were derived from the SJFCSP which was used as the basic of river dike construction. The field data of the cross section showed the relation between the distances (Y), interpreted as width of the cross section in SOBEK, and the vertical (Z). The Y-Z profile is opened cross section since the width of the surface level is larger than 10 mm. Figure 5-6 illustrates the Y-Z profile in Karanganyar River. The cross section was placed in every calculation point and the bed level was interpolated. There are several interpolation methods in SOBEK as illustrated in Figure 5-7.

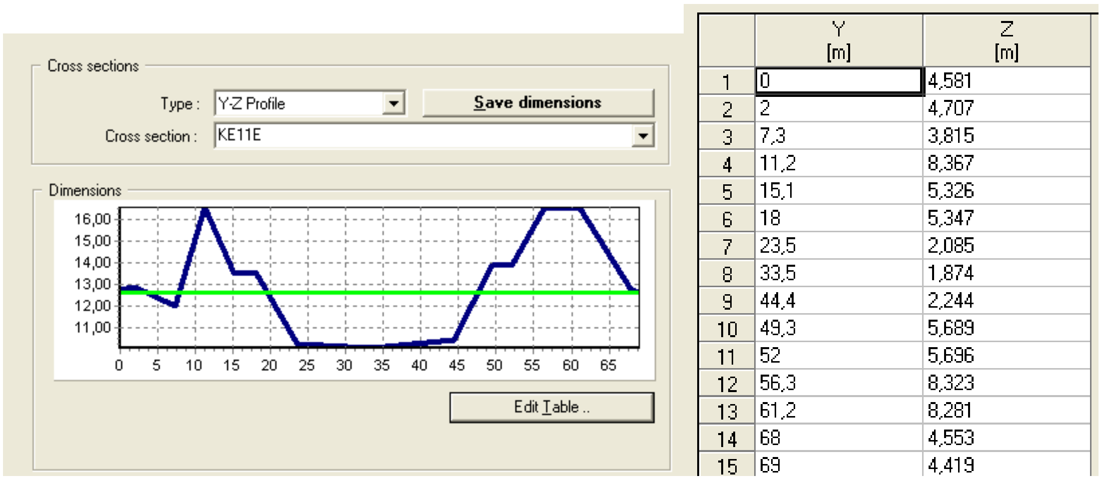

Figure 5-6. Y-Z profile used in 1D flow model

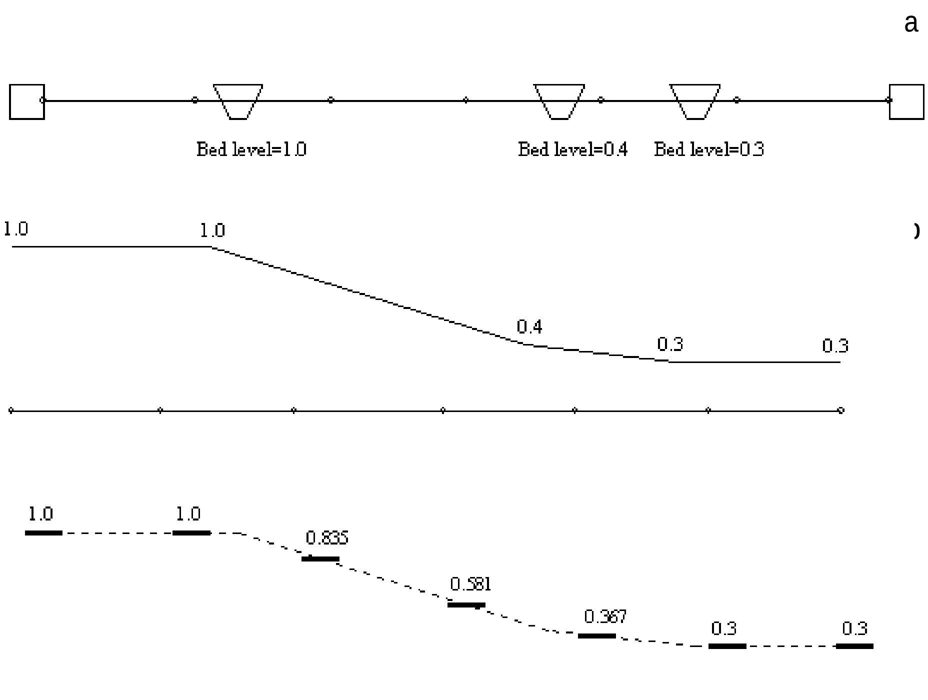

Figure 5-7. The interpolation and extrapolation method for cross section in SOBEK (a) the original cross section with different bed level (b) the linear and constant interpolation (c) the discrete interpolation and extrapolation (taken from SOBEK help)

5.2.3. Optimum DEM

For the purpose of the 2D modeling, an optimum DEM is required for the overland flow. The general and noisy DEM discussed in the previous chapter were used in this flood modeling. The optimum grid size was 50 meters and the DEM consists of 318 rows and 344 columns. To get closer with the flood situation in 2004, dike break scenario was set up. Based on the past flood data documented by the Public Work Office (unpublished) the width and height of dike break was 150 meters and 3 meters, respectively. Thus 6 pixels were lowered down 3 meters as the representation of the dike break (see Figure 5-8).

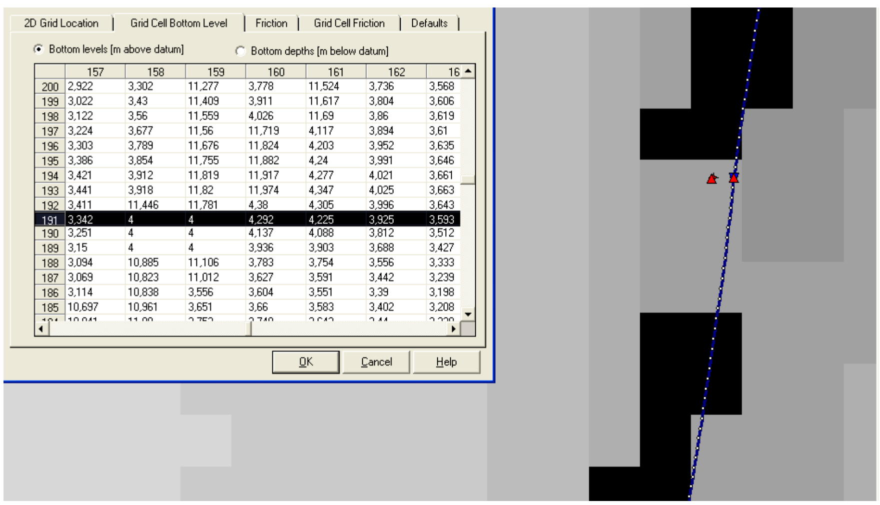

Figure 5-8. The DEM adjustment for dike break

5.2.4. Surface Roughness

Manning's n represents the resistance of the channel or floodplain to the flood flow. Surface roughness contributes to the flood model and is normally used to do the calibration. The surface roughness determines how the flood behaves either in the channel or on the floodplain. The type of the channel and the land use type of floodplain have a considerable contribution in the flood modeling. Land use type have been related to the flow behavior and translated into Manning's value (Manning's n). Surface roughness by using Manning's n has been implemented for medium to large catchment. Every land use type has specific surface structure and embed complex interaction due to the elevation change, surface irregularity, flow depth, vegetation density, scale, and obstructions (Kalyanapu, et al., 2009). Hence, Manning's n might be varied dependent on the land use type. The spatial distribution of the land use type is illustrated in Figure 5-9. These land use types was used t derive the Manning's n presented in Table 5-10.

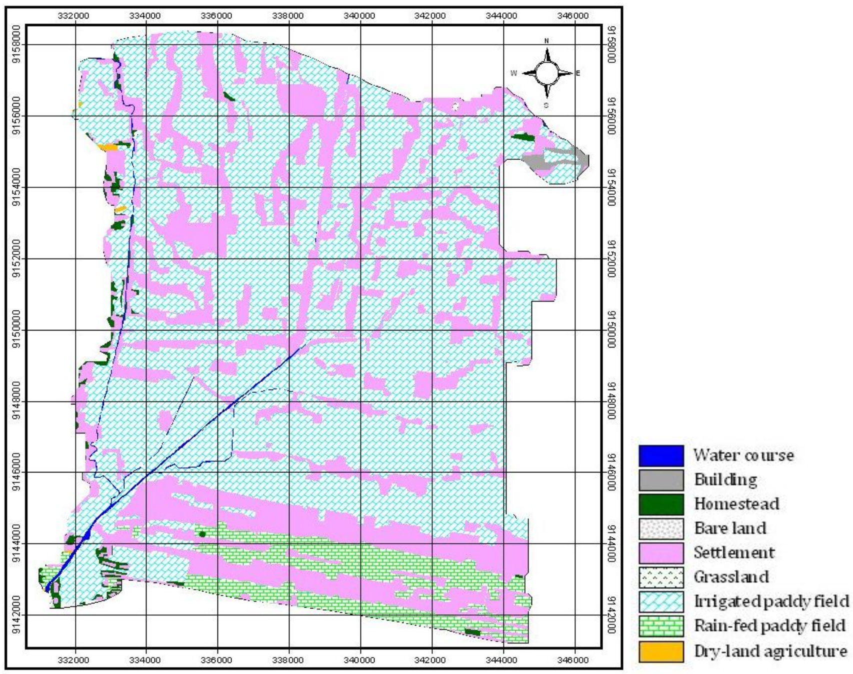

Figure 5-9. Land use type of the study area

Table 5-2. The Manning's n based on land use type

Land use type	Manning's n ($m^{1/3}s^{-1}$)
Bareland	0.020
Building	0.100
Dryland agriculture	0.035
Grassland	0.035
Homestead	0.035
Irrigated paddy field	0.030
Rain-fed paddy field	0.035
Settlement	0.100
Water course	0.010

5.3. Model Schematization

The flood model was set up or so-called schematization in SOBEK editing interface, NETTER. According to Alkema (2007), the boundary condition describes the exchange of water mass between the study area and the entire environment during the model run. In general, it can be explained how much water enters the study area in the upstream and how much water leaves through downstream. For the upstream boundaries, flow hydrograph (m^3/s) will be introduced (see Figure 5.10). Water level (m) is usually used in downstream boundary. Since the catchment outlet is located in the coastal area, thus 0 meter water level is preferred.

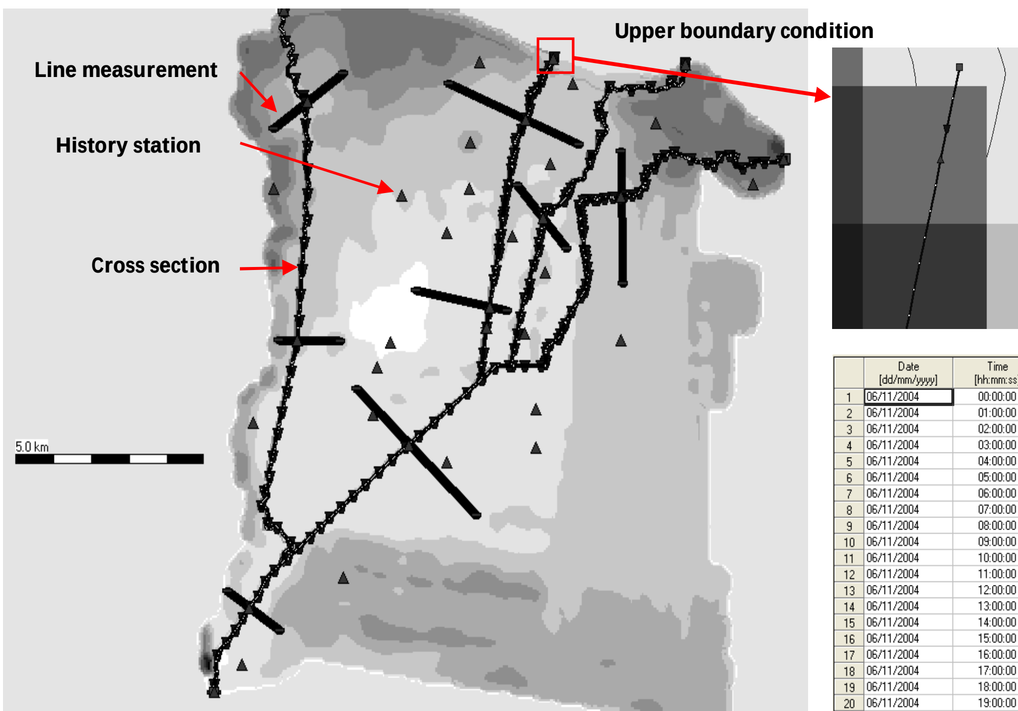

	Date [dd/mm/yyyy]	Time [hh:mm:ss]	Discharge [m3/s]
1	06/11/2004	00:00:00	0
2	06/11/2004	01:00:00	4,311761
3	06/11/2004	02:00:00	12,935
4	06/11/2004	03:00:00	36,949
5	06/11/2004	04:00:00	60,962
6	06/11/2004	05:00:00	84,976
7	06/11/2004	06:00:00	99,623
8	06/11/2004	07:00:00	114,27
9	06/11/2004	08:00:00	128,917
10	06/11/2004	09:00:00	127,8027
11	06/11/2004	10:00:00	126,6883
12	06/11/2004	11:00:00	125,574
13	06/11/2004	12:00:00	116,789
14	06/11/2004	13:00:00	108,004
15	06/11/2004	14:00:00	99,219
16	06/11/2004	15:00:00	89,70728
17	06/11/2004	16:00:00	80,19554
18	06/11/2004	17:00:00	70,68382
19	06/11/2004	18:00:00	63,61059
20	06/11/2004	19:00:00	56,53736
21	06/11/2004	20:00:00	49,46414
22	06/11/2004	21:00:00	45,31387

Figure 5-10. Setting up the boundary condition for the flood model

5.4. Model Calibration and Validation

In the study area, the calibration of the flood model was done through changing the channel and surface roughness. The channel roughness coefficients used in the calibration step were 0.025, 0.03, and 0.035. These values were selected by considering the type of channel. Coarse sand was the bed material of the channel in the study area of which the Manning's n is 0.025 to 0.035. For the surface roughness, SOBEK takes 0.03 as the default. In addition to this, 0.03 is still in range for the coarse sand bed material (Arcement & Schneider, 1994). The surface roughness was adjusted by 0.005 for all the land use type except the building and settlement (see Table 5-3). The different adjustment for building and settlement was related to the contribution of the impervious area to the flood model. The calibration was done by simulating the 25 yr flood based on three different combinations of channel and surface roughness (see Table 5-4).

Table 5-3. Manning's value adjustment for model calibration

Land use type	Initial Manning's n ($m^{1/3}s^{-1}$)	Adjusted Manning's n ($m^{1/3}s^{-1}$)
Bareland	0.020	0.025
Building	0.100	0.150
Dryland agriculture	0.035	0.040
Grassland	0.035	0.040
Homestead	0.035	0.040
Irrigated paddy field	0.030	0.035
Rain-fed paddy field	0.035	0.040
Settlement	0.100	0.150
Water course	0.010	0.015

Table 5-4. Channel and surface roughness combination to calibrate the model

	Initial run	Run 2	Run 3
Channel roughness	0.03 $m^{1/3}s^{-1}$	0.025 $m^{1/3}s^{-1}$	0.035 $m^{1/3}s^{-1}$
Surface roughness	Initial Manning's n	Adjusted Manning's n	Initial Manning's n

As indicated by Graph 5-8 tributes to flood depth and Graph 5-9 for the flood velocity, there was very small change in the flood behavior. The changing of building and settlement by 0.05 $m^{1/3}s^{-1}$ did not make any significant different. By changing the channel surface into 0.025 and using the adjusted Manning's, the run 2 performs the highest depth and the velocity. The flood depth was 1.20 m and the velocity was 0.25 m/s.

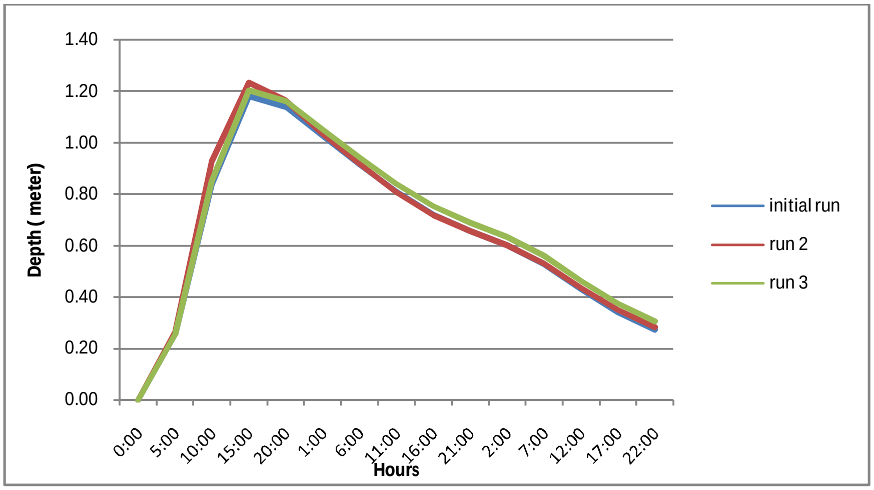

Graph 5-1. Comparison of the flood depth resulted from flood models using different channel roughness and surface roughness

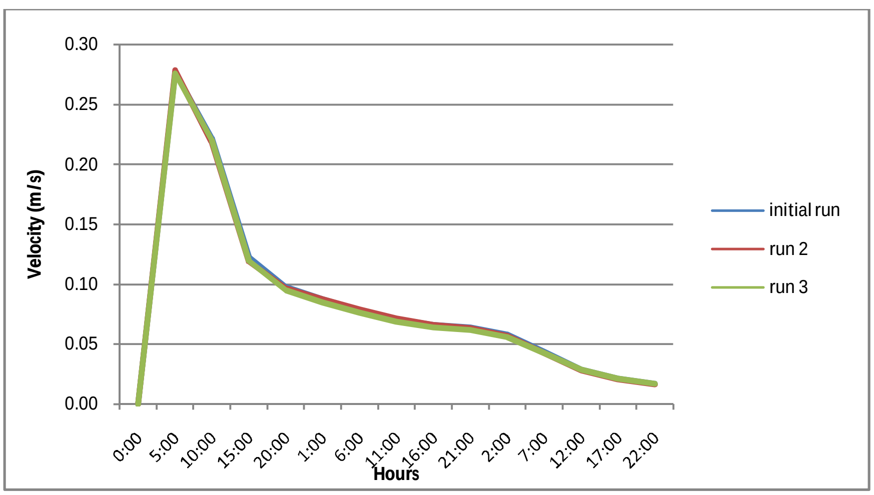

Graph 5-2. Comparison of the flood velocity resulted from flood models using different channel roughness and surface roughness

The available data of the past event flood in 2004 was only flood peak discharge and flood extent map. In addition to surface roughness adjustment, these two dataset were used to validate the flood model. The flood extent was mapped and updated through field survey. The modeled flood extent map was compared to the observed flood extent map. The validated flood extent map was shown by Figure 5-12. This comparison was also applied for the flood depth. The observed flood depth was derived from the interview with local community. The modeled and the observed flood extent show 43 km^2 differences which are quite significant (see Table 5-5). The 25 year flood model underestimates the flood extent in some areas. Comparing the spatial distribution of the observed and modeled flood extent, the underestimation is represented by the patchy structures.

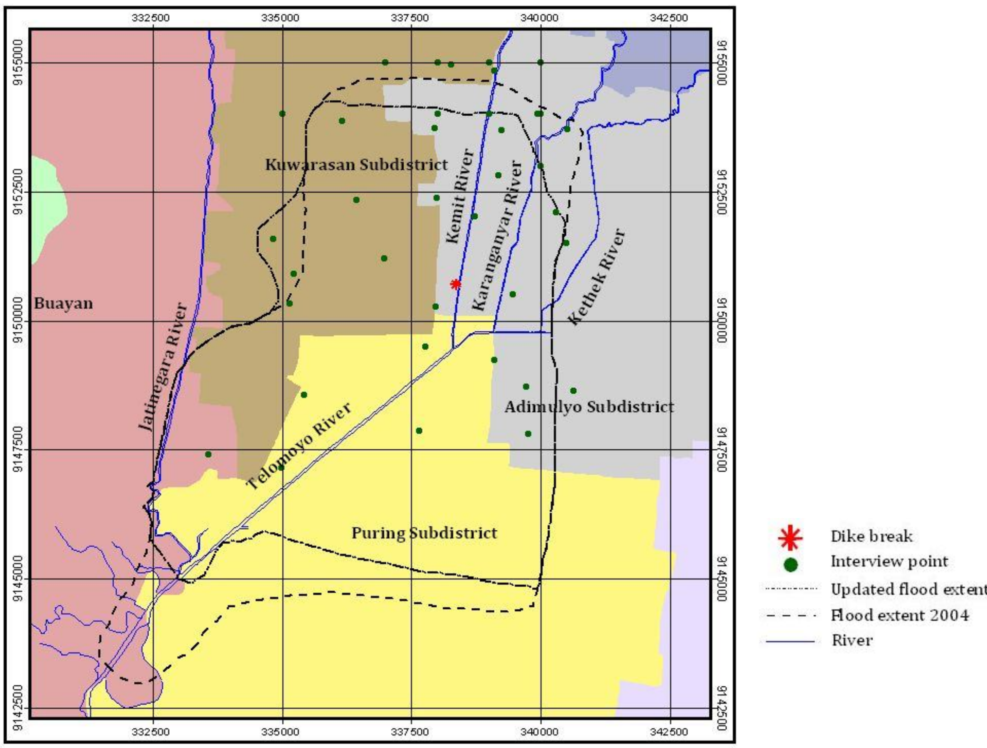

Figure 5-11. The validated flood extent map and the distribution the interview point

Table 5-5. The comparison of the observed and modeled inundation area

	Inundated (km2)	Not-inundated (km2)
Observed	66.44	214.33
Modeled	23.37	257.36
Difference	43.07	43.03
Total area	280.73	280.73

The comparison of the modeled and observed flood parameter was continued by comparing the flood depth. The flood depth was considered as the proper parameter to be compared since it is observable in the field. Flood depth was also remarkable for the local community. The initial run was deviate 0.35 m from the observed data and was just slightly different from the third run which deviated 0.38 m. Table 5-6 shows the comparison of the calibrated model and observed data. By changing the channel roughness into 0.025 has produced unidentified values represented as NA. The second run -0.31 m. By considering the distribution of the least flood depth deviation, the combination of the second run was selected to do the next analysis.

Table 5-6. The comparison of the observed and modeled flood depth

	Observed	Run 1	Diff 1	Run 2	Diff2	Run 3	Diff3
FW11	0.15	0.61	0.46	0.12	-0.04	0.22	0.07
FW12	0.15	0.03	-0.12	0.03	-0.12	0.19	0.04
FW18	0.15	1.34	1.19	0.09	-0.06	0.51	0.36
FW21	0.50	1.13	0.63	0.02	-0.48	1.35	0.85
FW24	0.50	0.67	0.17	0.02	-0.48	0.72	0.22
FW26	0.15	1.23	1.08	0.02	-0.13	1.25	1.10
FW27	0.15	0.34	0.19	NA	-0.15	0.42	0.27
FW28	0.15	1.08	0.93	NA	-0.15	1.10	0.95
FW31	0.50	1.13	0.63	NA	-0.50	1.20	0.70
FW32	0.50	1.48	0.98	NA	-0.50	1.52	1.02
FW34	0.15	0.70	0.55	0.02	-0.13	0.16	0.01
FW35	0.15	0.61	0.46	NA	-0.15	0.48	0.33
FW37	0.50	0.00	-0.50	NA	-0.50	1.39	0.89
FW37	0.70	1.25	0.55	NA	-0.70	1.39	0.69
FW44	0.50	0.26	-0.24	NA	-0.50	0.36	-0.14
FW45	1.00	0.01	-0.99	NA	-1.00	0.00	-1.00
FW47	0.15	0.14	-0.01	NA	-0.15	0.20	0.05
FW49A	0.50	0.44	-0.06	0.04	-0.46	0.38	-0.12
FW50	0.15	0.08	-0.07	NA	-0.15	0.36	0.21
FW51	0.15	1.03	0.88	NA	-0.15	1.07	0.92
FW52	0.14	0.73	0.59	0.11	-0.03	0.65	0.51
Mean			0.35		-0.31		0.38

5.5. Flood Model Output

5.5.1. Flood Extent

The first output of flood modeling is the flood extent. It shows the spatial distribution of the flood in the floodplain. In general, the inundated area is much less than not-inundated area. Graph 5-1 shows that higher return period of flood cause larger spatial distribution. The largest inundated area was caused by 25 year return period flood and it is covered less than 15% of the study area (see graph 5-2). In general the difference of the flood extent from low magnitude flood to high magnitude flood was not significant. The difference from the lowest magnitude (2yr) and highest magnitude was about 12 km^2 or 50% different. The flood extent caused by 5yr and 10yr flood was similar with less 1% different. The low elevation variation in the study area may contribute in the flood spatial distribution.

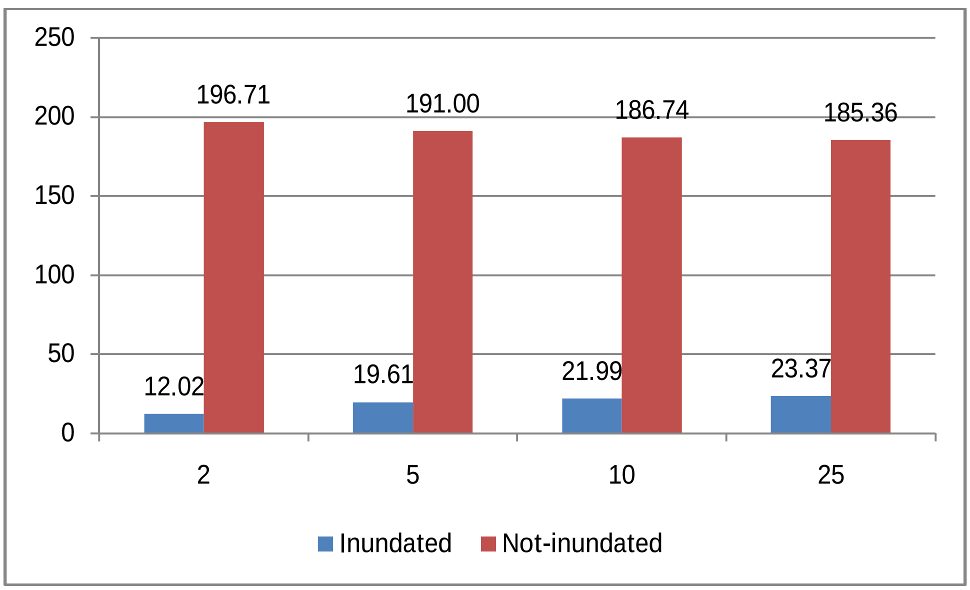

Graph 5-3. The comparison of inundated area and not-inundated area

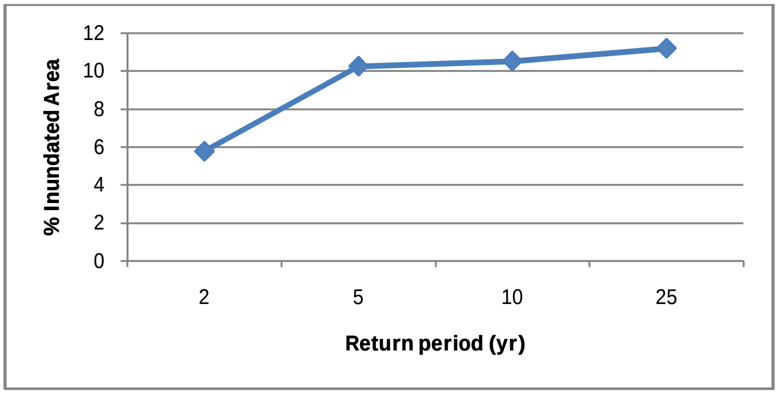

Graph 5-4. The inundation area increases as the flood magnitude increase

As was shown in graph 5-2 the inundation covers less than 15% of the areas for the highest magnitude flood (25 yr). The spatial distribution is shown in Figure 5-13. In general, the inundated area shows patchy structures due to the variation of the elevation. Small variation in the elevation obviously affects the flood distribution. The floodplain of Karanganyar and Ketek River were always inundated by either small magnitude flood or high magnitude flood. Unlike of two rivers in the west, floodplain of Kemit River started to be inundated by 5yr flood and increase as the higher flood magnitude occurred. The floodplain of Jatinegara River was never inundated due to the control of the Sempor Reservoir.

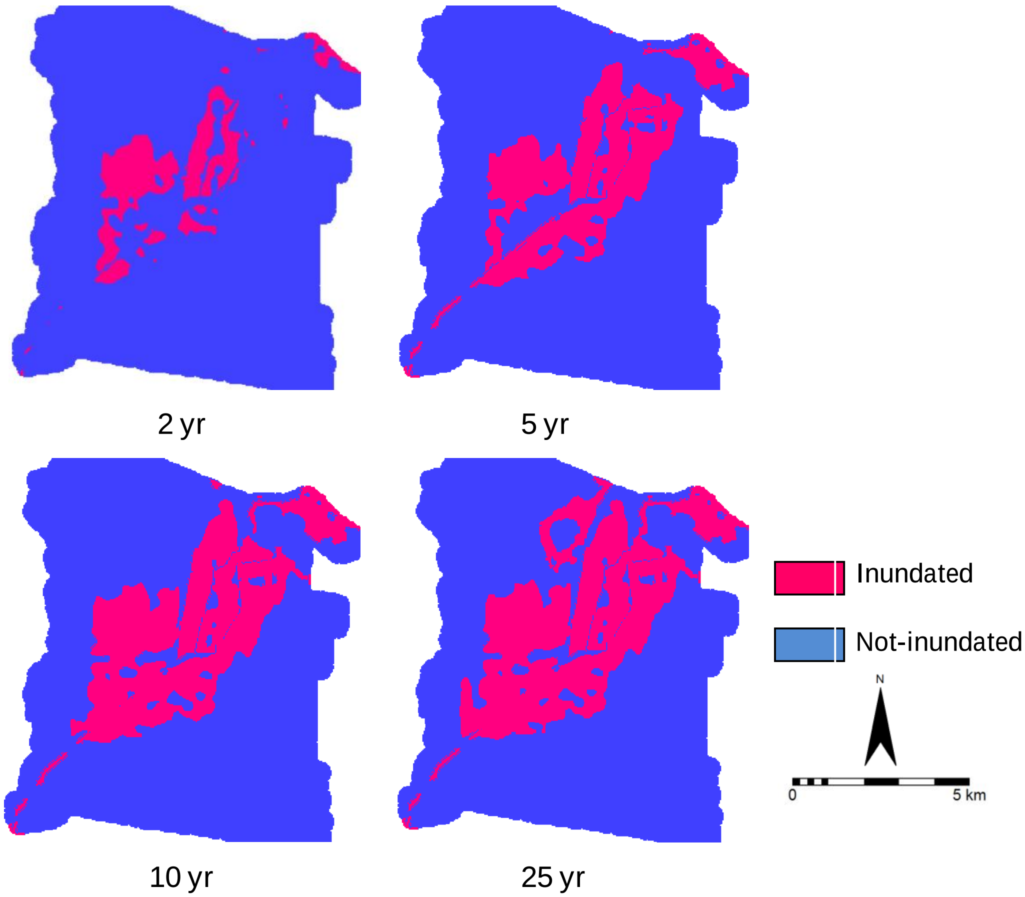

Figure 5-12. The modeled flood extent for 2 yr, 5 yr, 10 yr, and 25 yr

5.5.2. Flood Depth

The flood depth is varied by the elevation and the flood magnitude. The area in between Kemit and Karanganyar River is low elevation area thus the water from the two rivers overtops and inundates this area (see Figure 5-13). The depth of the inundation is more than 1 meter. The different flood magnitude may produce variation in the flood depth. As the probability of flood to occur decrease the flood depth is increasing. The deepest inundation recorded in station 1334 (area in between Kemit and Karanganyar River) was more than 1.2 meter. Significant change was found when 2 yr flood shifted to 5 yr flood or higher. The flood depth increased from 0.70 meter to 1.3 meters (see graph 5-13).

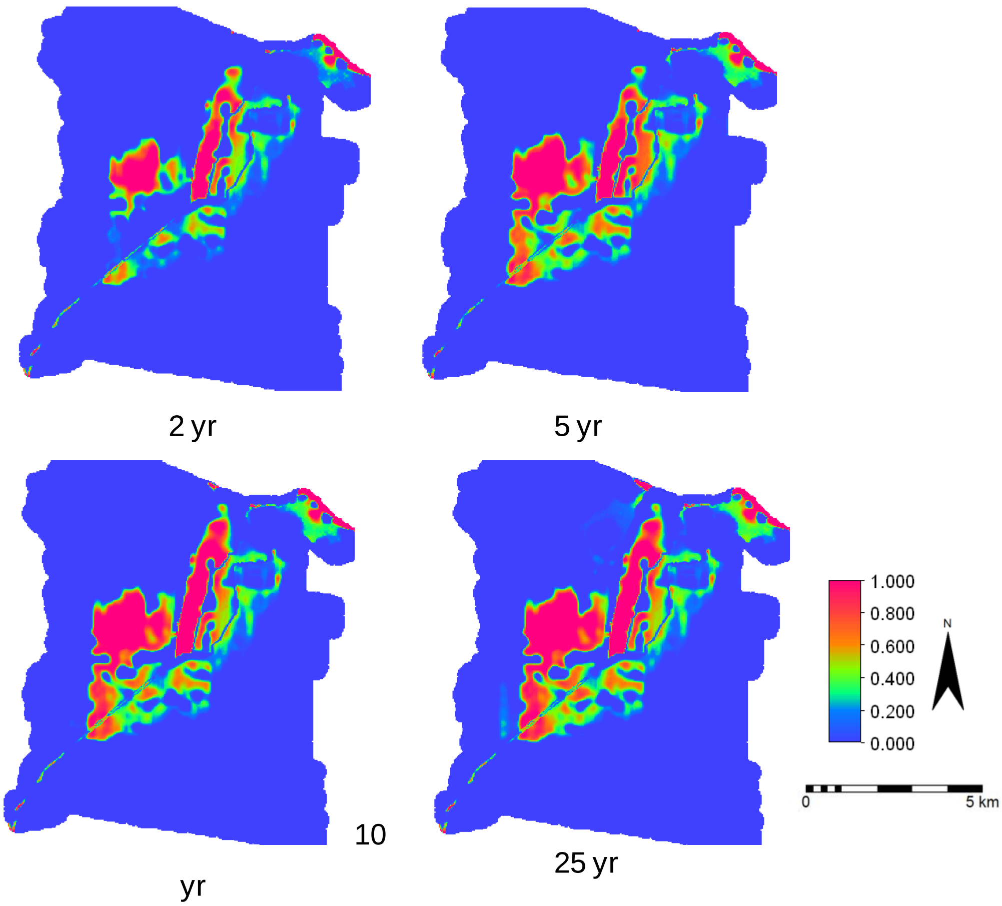

Figure 5-13. Spatial distribution of the modeled flood depth for 2 yr, 5 yr, 10 yr, and 25 yr flood

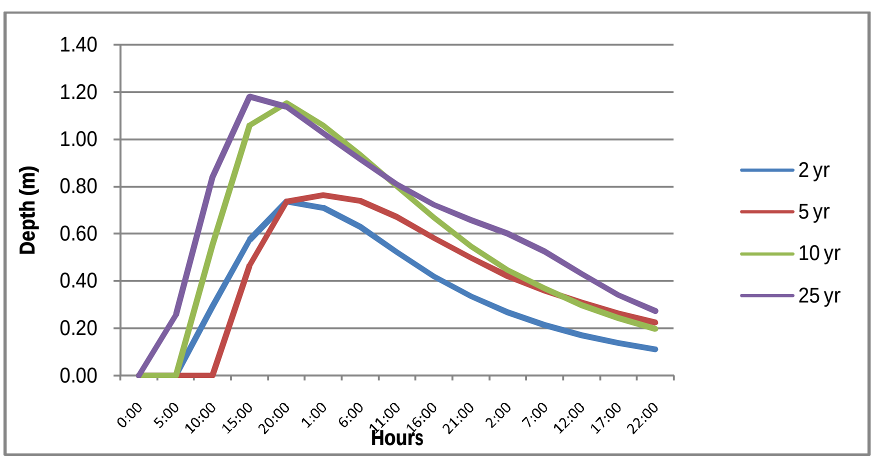

Graph 5-5. Temporal flood depth in the floodplain between Kemit and Karanganyar River (station 1334)

5.5.3. Flood Velocity

To analyze the flood parameter, flood velocity is essential due the energy in which is contained. The maximum velocity resulted by this model was ranged from 2.44 m/s for 2 yr flood to 2.77 m/s for the 25 yr flood. There was no significant change between the 5 and 10 yr flood. In general, the velocity is positively correlated with the flood magnitude. Greater flood creates higher velocity (see Graph 5-5).

The spatial distribution of the flood velocity was varied by the distance from the river. The high velocity took place in the northern part or the floodplain of Kemit, Karanganyar, and Ketek (see Figure 5-15). The settlement area located along the river increased the velocity due to the low friction. The floodplain of Telomoyo River which was occupied by irrigated paddy field behaved in adverse way. The velocity in this area was less due to the greater fiction of the surface.

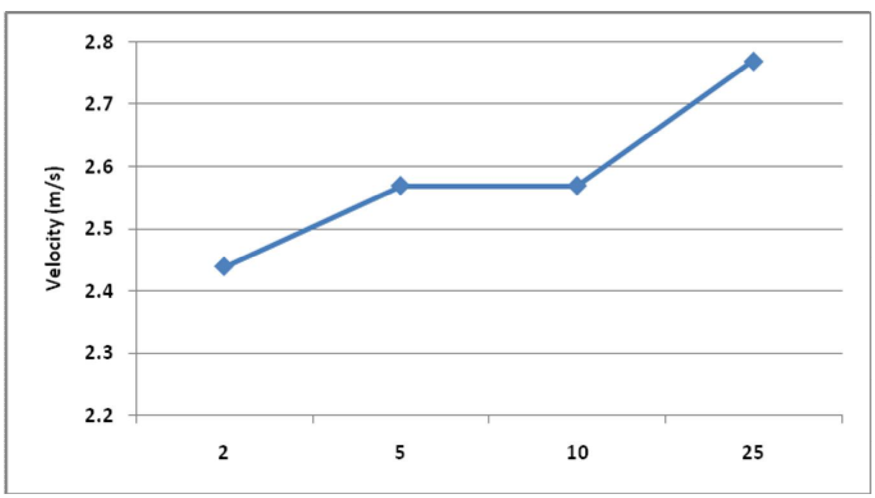

Graph 5-6. The increasing of flood velocity as the flood magnitude increased

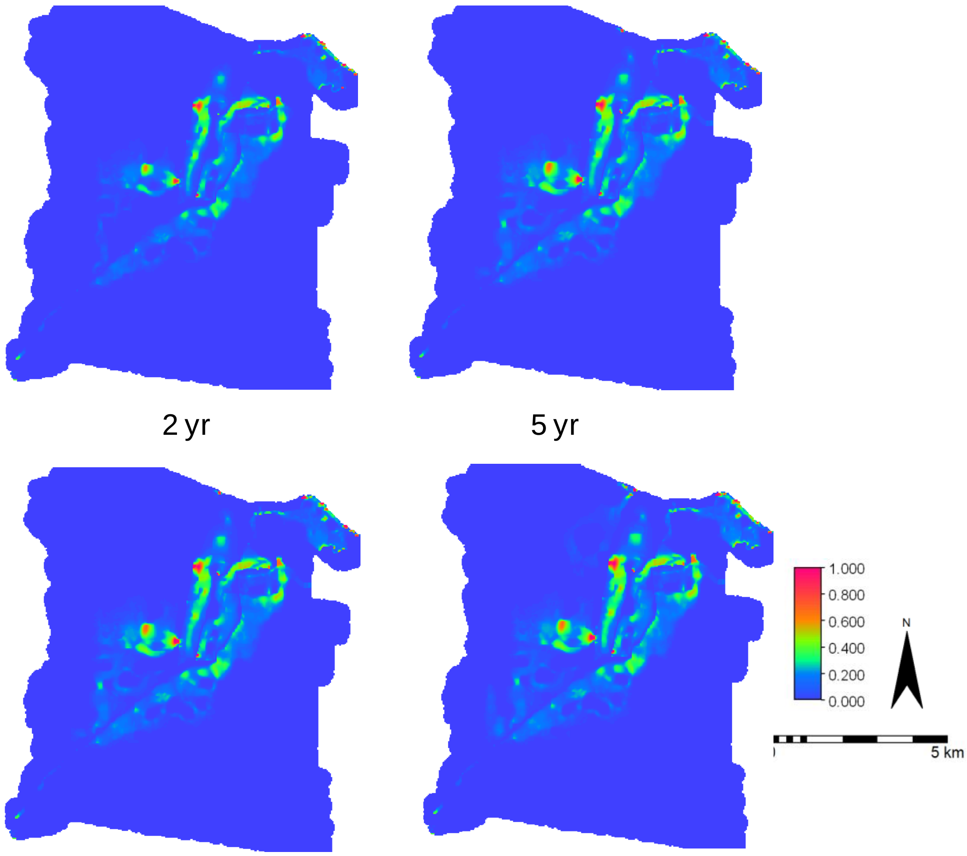

2 yr

5 yr

10 yr

25 yr

Figure 5-14. Spatial distribution of the flood velocity

The velocity recorded in the history station, shows the significant increase in the first five hours of the flood. In station 1331 which is located on the floodplain recorded that the overland flow for the 25 yr flood is increased by the time the water come and reach the peak within 5 hours (see graph 5-6). But the overland flow for smaller flood behaves in slightly different way. It is recorded that there was a little bit delay for the overland flow to reach the peak. The maximum velocity was reached after 10 hours. In this station, the recorded velocity was 0.25 m/s for the 2 yr flood and 0.255 m/s for the 25 yr flood.

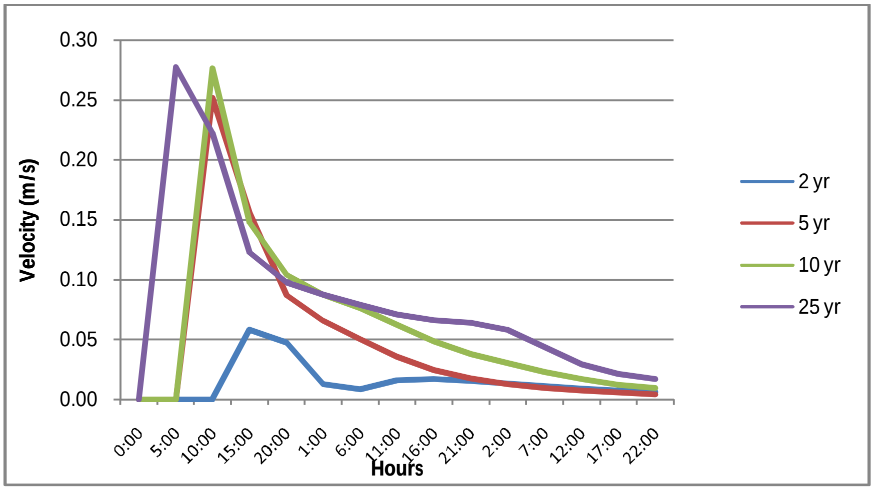

Graph 5-7. Temporal flood velocity in the floodplain of Kemit and Karanganyar River (station 1334)

5.5.4. Flood Impulse

To assess the amount of water movement in the floodplain, the flood depth and flood velocity were multiplied (Alkema & Middelkoop, 2005). The maximum impulse of the flood was found at edge of the study area as shown in the Figure 5-16.

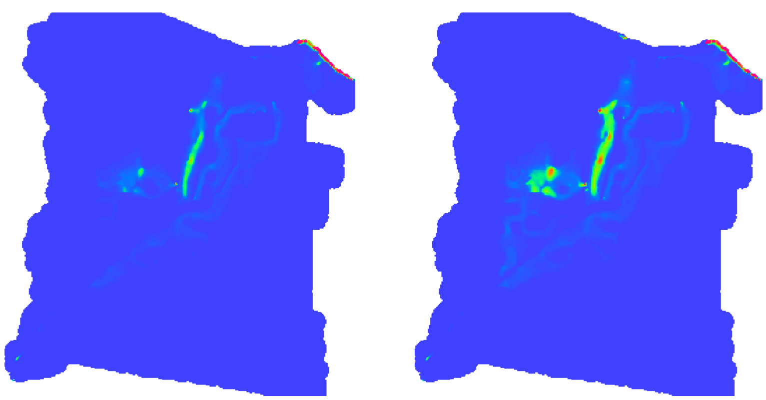

2 yr   5 yr

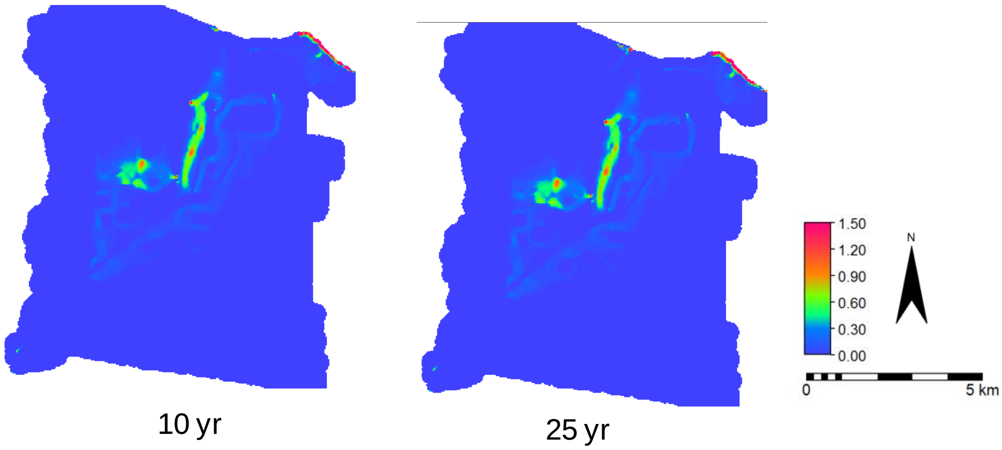

Figure 5-15. Spatial distribution of the flood impulse for 2 yr, 5 yr, 10 yr, and 25 yr flood

5.5.5. Flood Hazard

Flood hazard mapping can be done by taking flood depth and flood velocity in to account. Flood impulse as the product of multiplication of these two parameters draws the energy of the water movement. Deep inundating water with high velocity is considered as the destructive flood. Deep inundating water with low velocity has less energy to destruct and adversely, shallow inundating water with high velocity may have greater energy to destruct. As was shown in figure 5-17, the study area was dominated by low and medium flood hazard. The classification was based on the relationship between the average velocity and depth developed by Penning-Rowsell and Tunstall (1996). The flood average flood velocity of 2 m/sec with flood depth 1 m was the threshold for the high hazard. The flood hazard classification was based on Table 5-7. The low flood velocity and shallow inundating water in the floodplain reduce the impulse level.

Table 5-7. Hazard classification based on impulse

Impulse class	Hazard classification
0 – 0.1	Low hazard
0.1 – 1	Medium hazard
>1	High hazard

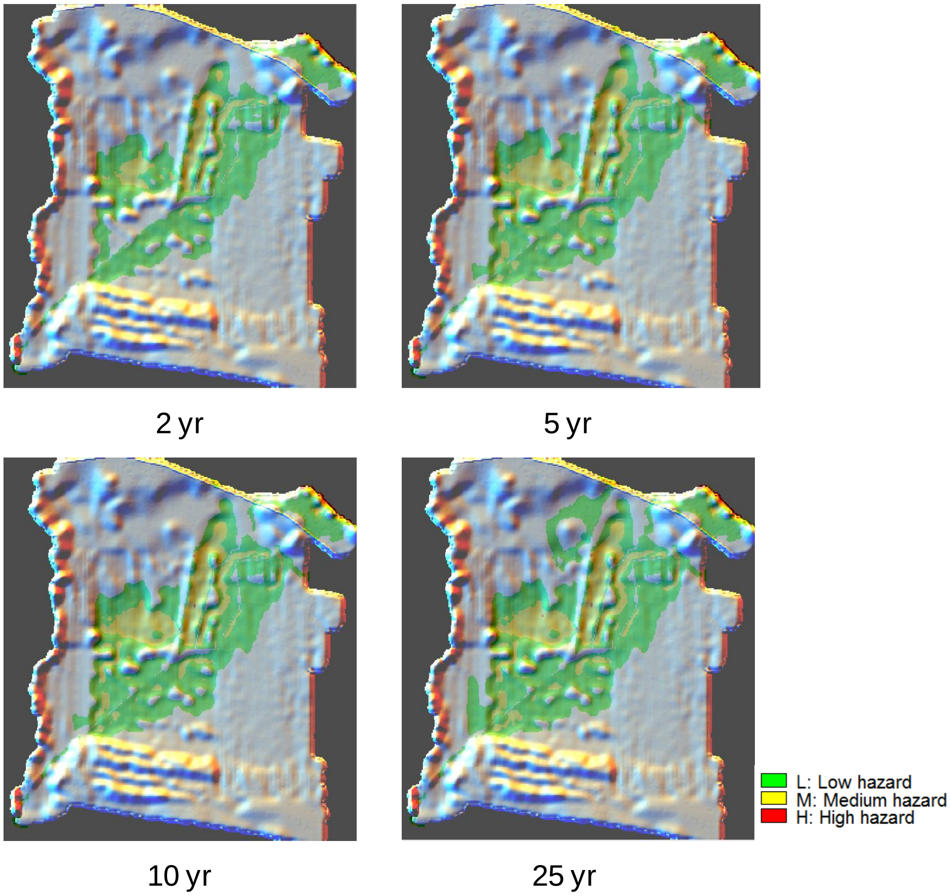

Figure 5-16. The flood hazard distribution based on different flood

Table 5-8. The distribution of the flood hazard

	Low hazard (Km^2)	Medium hazard (Km^2)	High hazard (Km^2)
2 yr	33.25	6.63	0.30
5 yr	37.05	12.42	0.33
10 yr	37.05	12.42	0.33
25 yr	42.45	13.29	0.41

6. DISCUSSION

6.1. DEM Generation

Working under limited available data was a challenge to justify the proper method that would be applied. Undocumented accuracy or error level of particular data required an approach to assess the accuracy before it was applied. To identify the accuracy of the elevation point, a photogrammetric related literature was reviewed to assume the nominal accuracy.

In general, this type of study is very dependent on the DEM accuracy. Thus the interpolation of elevation point should be as accurate as possible. The spacing of the elevation point of 100 m x 100 m limits the optimum grid size of the interpolation. To get rigid grid size, the existing elevation points should be integrated with another elevation point which has a better accuracy. Since the study area is a flat terrain, the point map derived from 1: 25000 scale of topographic map is not sufficient to be integrated with the existing elevation points due to sparse point spacing. The optimum grid size used in this study was 50 meter. Increasing the optimum grid size supposed to 20 or 10 meter would not be proper since inadequate terrain information.

The selection of the interpolation model was based on the decision tree developed by Bivand et al. (2008). Although the decision tree shows simple kriging was the proper method, another kriging method was tested in this study. The accuracy assessment showed that there was no significant different between the simple kriging, ordinary kriging, and regression kriging. The simple kriging has the lowest standard deviation thus this model was selected. The uncertainty of the DEM interpolation was represented by the variation. The variation of the interpolation was ranged from 5.3 cm to 1 meter.

The existing elevated road, apparently did not give any significant change to the model. It was expected that the road would be the freeway for the water flow. In fact, the asphalt thickness was not a good option for man-made integration to general DEM. Unless the

The integration of the elevated features and the DEM was aimed to obtain real-world representation. The elevated features used in this study were road, dike, and railways. The measurement of the roads and railways was only based on site visit and simple measurement using measuring tape. The dike height was derived from the SJFCSP secondary data. By adding the elevated features, the noise was introduced to interpolate DEM and the accuracy was reduced. The DEM accuracy and quality assessment excluded the elevated features since the elevated feature was not included in the interpolation process.

6.2. Flood Modeling

For the simulation purpose, the 24 hour designed flood hydrograph had to be extrapolated to 72 hour. The extrapolation was based on the linear form. The limitation of this method is lack of theoretical basis and can lead to the undesirable result (Boufadel, 1998). The extrapolation in this study has extended the time to peak for the water flow and the time base. This may increase the uncertainty of the model from the hydrological point of view.

Another uncertainty of the model was raised due to the placement of the upper and lower boundary. The distance of the boundaries should be sufficiently far from the DEM boundary. Too close from the DEM will overestimate the water due to short period of travel time and too far will underestimate the model due to longer travel time. It needs to be noted that the model assumes that the incoming water is only from the discharge. Thus the flood model may underestimate the amount of water since the ignorance of the water in small tributaries.

Calibration is an essential step in a modeling. In this study, the changing of the channel and surface roughness did not give a significant different. This may be due to the homogeneity of the land use type and also the slope variation. The domination of particular land use type such as irrigated paddy field limit the number of alternatives in changing the Manning's n. The increasing of Manning's values for settlement and building up to 0.150 $m^{1/3}s^{-1}$ did not make a considerable change because of the effect of low slope variability.

The past event flood extent map was assumed to have at least 5 meter accuracy due to it was produced by hand held GPS. The flood extent map suffered from the effect of generalization. The spatial variation of the elevation was not taken into account thus the the flood seemed to be inundated the entire study area. In fact, micro topography of the area does exist and affect the flood distribution. Considering this limitation, the difference of the flood extent which reached 43 km2 was not surprisingly result.

The past flood event in 2004 was suffered from the uncertainty. Digging the flood depth information from the local community was rather difficult. Collecting the exact depth was impossible, the local community use part of their body as the depth reference instead. Hence, the transformation the flood depth was using the average.

7. CONCLUSION AND RECOMMENDATION

7.1. Conclusion

This study was carried out to address some questions that were related to the objectives. The conclusion was the answer of the raised questions.

Which interpolation method gives the best result for the DEM generation?
How should the error of interpolated DEM be assessed?

The geostatistical analysis found that the simple kriging is able to perform the best result for the DEM generation. This is based on the accuracy assessment of which the simple kriging has the least standard deviation (2.98 m), RMSE (0.31 m), and bias (-0.01).

The use of standard deviation, RMSE, and bias could explain the error of DEM prediction. These parameters showed the deviation of model from the real values.

Which areas are to be likely inundated by the different return period floods?
What is the significant change of flood behavior with the changing the different return period?

The areas behind the dike of Kemit, Karanganyar, and Kethek River are to be likely inundated by all different return period of flood. The floodplain adjacent the Jatinegara River was least probable to be inundated since the control of the Sempor Reservoir. Be specific

The flood extent indeed is the obvious change of flood behavior. The higher magnitude of flood the wider flood extent would be. The velocity of Kemit River was significantly changing from 2 yr flood to 5 yr flood. The peak velocity changed from 0.05 m/s to 0.25 m/s.

Is there any systematic pattern of the flood extent for the different return period?

Flood model for the different return periods did show the systematic pattern of the flood extent. The increase of the flood magnitude has enlarged the flood extent; however the main pattern remained to exist.

7.2. Recommendation

The DEM error propagation in flood modeling is an interesting research topic. There are many uncertainty of the flood modeling which is left uninvestigated in this study. Several recommendations are proposed for the next research as listed below.

1) This study used elevation point with 100 m spacing and not detailed enough to represent the topography and the man made feature on the terrain. Thus more detailed DEM is required. The building footprint needs to be integrated due to its essential contribution in the flood propagation.
2) More detail hydrological data is required since the flood is affected by one single event of rain. The daily rainfall and discharge were not adequate to represent the rainfall-runoff model.
3) The geomorphological process takes place in the upper stream such as the erosion should be considered in the flood modeling since the river capacity is very much dependent on the amount of the deposition in the river itself. The deposition along the river affects the river cross section and also the channel roughness.

8. References

ADB. (2007). *Indonesia: South Java Flood Control Sector Project* (No. 29312): Asian Development Bank.

Alkema, D. (2007). *Simulating floods : on the application of a 2D-hydraulic model for flood hazard and risk assessment.* ITC, S.l.

Alkema, D., & Middelkoop, H. (2005). The Influence of Floodplain Compartmentalization on Flood Risk within the Rhine-Meuse Delta. *Natural Hazards, 36*, 125 - 145.

Apel, H., Thieken, A. H., & Blöschl, G. (2004). Flood Risk and Associated Uncertainty. *Natural Hazards and Earth System Sciences, 4*, 295 - 308.

Arcement, G. J., & Schneider, V. R. (1994). Guide for Selecting Manning's Roughness Coefficients for NAtural Channels and Flood Plains. *United States Geological Survey Water-supply Paper, 2339*.

Ardiansyah, P. O. D., & Yokoyama, R. (2002). DEM Generation Method from Contour Lines Based on The Steepest Slope Segment Chain and a Monotone Interpolation Function. *ISPRS Journal of Photogrammetry and Remote Sensing, 57*, 86 - 101.

Bates, P., Anderson, M., Price, D., Hardy, R., & Smith, C. (1996). Analysis and development of hydraulic models for floodplain flows. *Floodplain processes*, 215–254.

Bates, P. D., & Roo, A. P. J. D. (2000). A simple raster-based model for flood inundation simulation. [doi: DOI: 10.1016/S0022-1694(00)00278-X]. *Journal of Hydrology, 236*(1-2), 54-77.

BCEOM. (2003). *South Java Flood Control Sector Project: Revised of Hydrology Report*: Ministry of Settlement and Regional Infrastructure.

Bivand, R. S., Pebesma, E. J., & Gomez-Rubio, V. (2008). *Applied Spatial Data Analysis with R*: Springer.

Blomgren, S. (1999). A Digital Elevation Model for Estimating Flooding Scenarios at The Falsterbo Peninsula. *Environmental Modeling and Software, 14*, 579 - 587.

Boufadel, M. C. (1998). Unit Hydrographs Derived from the Nash Model. *Water Resources Bulletin, 34*(1), 167 - 177.

Casas, A., Benito, G., Thorndycraft, V. R., & Rico, M. (2006). The topographic data source of digital terrain models as a key elements in the accuracy of hydraulic flood modelling. *Earth Surface Processes and Landforms, 31*, 444-456.

Chaplot, V., Darboux, F., Bourennane, H., Leguédois, S., Silvera, N., & Phachomphon, K. (2006). Accuracy of interpolation techniques for the derivation of digital elevation models in relation to landform types and data density. *Geomorphology, 77*(1-2), 126-141.

Crosetto, M. (2002). Calibration and validation of SAR interferometry for DEM generation. *ISPRS Journal of Photogrammetry and Remote Sensing, 57*(3), 213-227.

de Smith, M. J., Goodchild, M. F., & Longley, P. A. (2006). Geospatial Analysis - a Comprehensive Guide to Principles, Techniques, and Software Tools. Retrieved 7 February 2011, from www.spatialanalysisonline.com

Desmet, P. J. J. (1997). Effects of Interpolation Errors on The Analysis of DEMs. *Earth Surface Processes and Landforms, 22*, 563 - 580.

Fisher, P. (1998). Improved Modeling of Elevation Error with Geostatistics. *GeoInformatica, 2*(3), 215-233.

Fisher, P. F., & Tate, N. J. (2006). Causes and consequences of error in digital elevation models. *Progress in Physical Geography, 30*(4), 467.

Frank, A., Ostan, A., Coccato, M., & Stelling, G. S. (2007). Use of integrated one-dimensional/two dimensional hydraulic modeling approcah for flood hazard and risk mapping. *SOBEK Publication*.

Gao, J. (2001). Non-Differential GPS as an Alternative Source of Planimetric COntrol for Rectifying Satellite Imagery. *Photogrammetric Engineering and Remote Sensing, 67*(1), 49 - 55.

Hall, J., & Solomatine, D. (2010). A Framework for Uncertainty Analysis in Flood Risk Management Decisions. *INternational Journal of River Basin Management, 6*(2), 85 - 98.

Hartkamp, A. D., De Beurs, K., Stein, A., & White, J. W. (1999). *Interpolation Techniques for Climate Variables*. Mexico.

Hengl, T. (2007). *A Practical Guide to Geostatistical Mapping of Environmental Variables*. Italy: Instittute for Environment and Sustainability.

Holmes, K. W., Chadwick, O. A., & Kyriakidis, P. C. (2000). Error in a USGS 30-meter digital elevation model and its impact on terrain modeling. [doi: DOI: 10.1016/S0022-1694(00)00229-8]. *Journal of Hydrology, 233*(1-4), 154-173.

Horritt, M. S., & Bates, P. D. (2001). Predictng floodplain inundation: raster-based modelling versus the finite-element approach. *Hydrological Process, 15*, 825-842.

Hunter, G. J., & Goodchild, M. F. (1997). Modeling the Uncertainty of Slope and Aspect Estimates Derived from Spatial Databases. *Geographical Analysis, 29*(1), 35 - 49.

Hunter, G. J., & Goodchild, M. F. (1997). Modeling the uncertainty of slope and aspect estimates derived from spatial databases. *Geographical Analysis, 29*(1), 35-49.

Jonkman, S. N., Kok, M., & Vrijling, J. K. (2008). Flood Risk Assessment in the Netherlands: A Case Study for Dike Ring South Holland. *Risk Analysis, 28*(5), 1357-1373.

Kalyanapu, A. J., Burian, S. J., & McPherson, T. N. (2009). Effect of Land Use-based Surface Roghness on Hydrologic Model Output. *Spatial Hydrology, 9*(2), 51 - 71.

Kundzewicz, Z. W., & Menzel, L. (2003). *Flood Risk and Vulnerability in the Changing World*. Paper presented at the International Conference "Towards Natural Flood Reduction Strategies".

Lagacherie, P., Moussa, R., Cormary, D., & Molenat, J. (1996). *Effects of DEM Data Source and Sampling Pattern on Topographical Parameters and on Topography-based Hydrological Model.* Paper presented at the Application of Geographic Information Systems in Hydrology and Water Resources Management, Vienna.

Li, J., & Heap, D. (2008). A Review of Spatial Interpolation Methods for Environmental Scientists. *Geoscience Australia, 23*.

Liu, X. (2008). Airborne LiDAR for DEM Generation: Some Critical Issues. *Progress in Physical Geography, 32*(1), 31 - 49.

Neuhold, C., Stanzel, P., & Nachtnebel, H. P. (2009). Incorporating River Morphological Changes to Flood Risk Assessment: Uncertainties, Methodology, and Application. *Natural Hazards and Earth System Sciences, 9*, 789 - 799.

Paquet, R. (2010). *Estimation of interpolation errors in DEMs using statistical method*. Paper presented at the FIG Congress. Retrieved from www.fig.net/pub/fig2010/papers/fs02d%5Cfs02d_paquet_3985.pdf

Prachansri, S. (2007). *Analysis of soil and land cover parameters for flood hazard assessment : a case study of the Nam Chun watershed, Phetchabun, Thailand.* ITC, Enschede.

Raaflaub, L. D., & Collins, M. J. (2006). The effect of error in gridded digital elevation models on the estimation of topographic parameters. [doi: DOI: 10.1016/j.envsoft.2005.02.003]. *Environmental Modelling & Software, 21*(5), 710-732.

Savitri, E. (2006). *The Use of GIS and Remote Sensing to Identify Areas at Risk from Erosion in Indonesian Forests: A Case Study in Central Java.* Massey University, Palmerstone North, New Zealand.

Smith, K., & Ward, R. (1998). *Floods: Physical Processes and Human Impacts*. West Sussex, England: John Wiley and Sons Ltd.

Team, A. G. V. (2009). *ASTER Global DEM Validation*. Japan: ERSDAC.

UN-OCHA. (2010). *Pakistan: Initial Floods Emergency Response Plan*: United Nations Office for the Coordination of Humanitarian Affairs.

Wechsler, S. P. (1999). *Digital Elevation Model (DEM) uncertainty: evaluation and effect on topographic parameters*.

Wechsler, S. P. (2003). Perceptions of digital elevation model uncertainty by DEM users. *URISA Journal, 15*(2), 57.

Wechsler, S. P. (2007). Uncertainties Associated With Digital Elevation Models for Hydrologic Applications: a Review. *Hydrology and Earth System Sciences, 11*, 1481 - 1500.

Wechsler, S. P., & Kroll, C. N. (2006). Quantifying DEM Uncertainty and its Effect on Topographic Parameters. *Photogrammetric Engineering and Remote Sensing, 72*(9), 1081 - 1090